Hindawi
Adsorption Science & Technology
Volume 2022, Article ID 4438286, 21 pages
https://doi.org/10.1155/2022/4438286

Review Article

A Methodical Review on Carbon-Based Nanomaterials in Energy-Related Applications

Robert Birundu Onyancha[1], **Kingsley Eghonghon Ukhurebor**[2], **Uyiosa Osagie Aigbe**[3], **Otolorin Adelaja Osibote**[3], **Heri Septya Kusuma**[4] and **Handoko Darmokoesoemo**[5]

[1]*Department of Technical and Applied Physics, School of Physics and Earth Sciences Technology, Technical University of Kenya, P. O. Box 52428-, 00200 Nairobi, Kenya*
[2]*Department of Physics, Faculty of Science, Edo State University Uzairue, PMB 04, Auchi, 312101 Edo State, Nigeria*
[3]*Department of Mathematics and Physics, Faculty of Applied Sciences, Cape Peninsula University of Technology, P.O. Box 1906, Cape Town, South Africa*
[4]*Department of Chemical Engineering, Faculty of Industrial Technology, Universitas Pembangunan Nasional Veteran Yogyakarta, Sleman, Indonesia*
[5]*Department of Chemistry, Faculty of Science and Technology, Airlangga University, Mulyorejo, Surabaya 60115, Indonesia*

Correspondence should be addressed to Robert Birundu Onyancha; 08muma@gmail.com

Received 16 January 2022; Revised 15 March 2022; Accepted 16 April 2022; Published 2 May 2022

Academic Editor: Jeevan Kumar Reddy Modigunta

Carbon nanomaterials are endowed with novel and magnificent optical, electrical, chemical, mechanical, and thermal properties, with a promising prospect in different advanced applications such as electronics, batteries, capacitors, wastewater treatment, membranes, heterogeneous catalysis, and medical sciences. However, macroscopic synthesis of carbon materials for industrial use has been a great challenge. Furthermore, structural nonhomogeneity and indefinite fabrication have hindered vigorous and consistent implementation of these materials in extensive technologies. Nevertheless, they offer exotic physics, and as a result, they have continued to attract great interest from the scientific community in an effort aimed to optimize their properties through innovative synthesis techniques, ensuring macroscopic production and discovering new applications. Hence, this study endeavours to provide a conscious review of these materials via the comprehensive discussion of the various allotropes of carbon (fullerenes, carbon nanotubes, and graphene), synthesis techniques (arc discharge, laser ablation, and chemical vapor deposition), and their applications in energy-related fields (batteries, capacitors, photocells, hydrogen storage, sensors, etc.) and their impending prospects.

1. Introduction

The well-known carbon, with 6 electrons, is composed of four external shell electron orbitals (2s, $2p_x$, $2p_y$, and $2p_z$) and as a result can hybridize into sp^1, sp^2, and sp^3. These configurations present carbon as the most intriguing element known in the universe. Owing to its allotropic characteristics, it forms compounds that have varied properties dependent on the adjacent arrangement of carbon atoms. Naturally, diamond and graphite are considered the natural allotropes of carbon with diamond exhibiting sp^3 hybridization with a bond length of 1.56 Å. Conversely, graphite hybridizes in sp^2 with a hexagonal (honeycomb) lattice, with a bond length of 1.42 Å, and carbon inter-layer spacing of 3.35 Å [1].

In the recent past, studies have revealed new allotropes of dimensions: zero-dimensional (0-D) fullerenes, one-dimensional (1-D) carbon nanotubes (CNTs), and two-dimensional (2-D) graphene nanomaterials (NMs). Graphene is considered a monoplanar sheet of sp^2-bonded carbon atoms in a honeycomb crystal lattice, and it is a structural element for other forms of carbon allotropes. For example, the rolled-up graphene results in the formation of CNTs, but when curled up, it forms fullerenes. Fullerenes

(regularly known as molecular carbon) are an asymmetrical sheet of sole-atom-thick sheet graphite curled up to form a sphere consisting of pentagons and hexagons. Alternatively, CNTs are seamless cylindrical tubes with a diameter range of 1-100 nm and can be grouped into two: single-walled CNTs (SWCNTs) and multiwalled CNTs (MWCNTs). SWCNTs are perceived as a single-graphene layer of length range of 1-100μm rolled up whereas MWCNTs are nested concentric shells of SWCNTs with a spacing of 3.4 Å between individual walls [2, 3].

The characteristics of these carbon-based NMs are dependent strappingly on their atomic structures and relations with other materials [4]. Compared with conventional materials, carbon-based NMs possess excellent optical, electrical, mechanical, and surface area to volume ratio properties [5]. Therefore, these materials have attracted great interest from science and industries due to the novelty in properties that are auspicious for several advanced applications in areas like electronics, batteries, capacitors, wastewater treatment, membranes, heterogeneous catalysis, tissue reengineering, drug delivery, imaging, and biosensing [5, 6].

Imperatively, the properties and applications of NMs are immensely influenced by the dimensions, morphologies, and forms of carbon. Consequently, the synthesis of these materials with the anticipated properties has received substantial consideration. Thus far, a plethora of synthesis techniques such as chemical vapor deposition (CVD), arc discharge and laser, electrolysis, hydrothermal, thermal decomposition, epitaxial growth on electrically insulated surfaces, unzipping of CNTs, and Hummer's method [2, 7] have been explored. Arc discharge, laser ablation, and CVD have been the predominant synthesis techniques.

Therefore, this review covers the following aspects of carbon NMs: a discussion on the three allotropes of carbon (fullerenes, CNTs, and graphene), common synthesis methods (arc discharge, laser ablation, and CVD), and the highlight of energy-related applications (Figure 1).

2. Carbon Nanomaterials

In the foregoing section, albeit in brief, we have conversed on carbon NMs such as fullerene, CNTs, graphene, nanofibers, and nanodiamonds. Interestingly, this area has a record of three main scientific awards, i.e., the two distinguished Nobel Prizes for the discovery of fullerene and graphene together with the Kalvin prize awarded in the discovery of CNTs. The scientific interest in these materials is immense owing to their exceptional properties which have prompted a widespread application.

From being used in water treatment, biomedicine (drug delivery, chemotherapy during cancer treatment, antiviral activity, and biosensors), electronics, energy, and nanotechnology, these materials have in no doubt improved and changed every industry in which they have been implemented. As a result, there has been swift research development in the science and technology of carbon NMs over the past two decades that has culminated in the accumulation of an enormous amount of knowledge on these materials in terms of properties and mechanisms. A fact that can be proved by ten thousand publications, academic talks, conferences, and forum lectures. Therefore, the focus of this chapter will be on fullerene, CNTs, and graphene as summarized in Figure 2.

2.1. Fullerenes. Fullerene is a 0-D nanomaterial that consists entirely of carbon atoms and occurs in spherical (Buckyball), ellipsoidal, or tubular (Bucky tubes or CNTs) forms. It was first predicted in 1970 by Osawa [8] and experimentally discovered in 1985 by Kroto et al. [9] who went on to be awarded the Nobel prize in chemistry in 1996 [10, 11]. It was synthesized via a laser vaporization technique under an inert atmosphere. The analysis revealed that the fullerene, C_{60} (Figure 3), formed, had 12 pentagonal and 20 hexagonal rings facing symmetrically and reminiscent of graphite. The C_{60} which contains 60 carbon atoms is often known as Buckyball (resembles soccer ball), a name derived from a geodesic dome designed by Buckminster Fuller. The nucleus-to-nucleus diameter and centre-to-centre distance between neighbouring molecules are about 7.1 Å and 10 Å, respectively [12].

Despite this outstanding discovery, physicochemical studies on fullerene were not possible until 1990 when Krätschmer et al. devised a simple technique to synthesize large and usable quantities of C_{60} [14]. They vaporized graphite rods under helium (He) atmosphere through the arc vaporization technique. Notably, at the cold surface of the reactor, they witnessed the condensation of soot. Then, soot was collected and boiled in an organic solvent (toluene, benzene, and xylene). Finally, evaporation was conducted to remove the solvents thus leaving behind a black condensate. Subsequently, conventional spectroscopic procedures were employed to study the characteristics of C_{60} which led to the discovery and synthesis of other fullerenes with a distinctive number of faces with C ranging from 20 to hundreds (Figure 4) which was achieved.

For example, C_{60}, C_{70}, C_{76}, and C_{84} have been found in soot and others synthesized via the flow of electricity in the environment [13]. The C_{60} is purple or violet colour with a molar mass (g/mol) of 720.6, C_{70} is brick red and has a molar mass (g/mol) of 840.7, C_{76} is light yellow-green with a molar mass (g/mol) of 912.76, C_{84} is brown and molar mass (g/mol) of 1008.84, and C_{86} has a molar mass (g/mol) of 1032.86 and is olive-green [15]. Some of the features of fullerenes are as follows: (i) fullerenes such as C_{76}, C_{78}, C_{80}, and C_{84} are inherent chiral due to the D_2-symmetry; (ii) C_{60} does not show super-aromaticity; (iii) with an exception of small ones, fullerenes are stable; (iv) they are sparing soluble in many solvents; (v) their toxicity depends on the type, functional group of solvent, and synthesis method used [12].

2.1.1. Structure and Symmetry of Fullerenes. Fullerenes have a cage-like structure and exhibit 5-fold symmetry. To avoid localization of the strain resulting from sp^2 hybridization of carbon atoms, a separation of the five-member rings is needed. All the fullerenes discovered thus far have even numbers of carbon atoms and are described by general formula C_{20+2H} (H being the number of hexagonal faces)

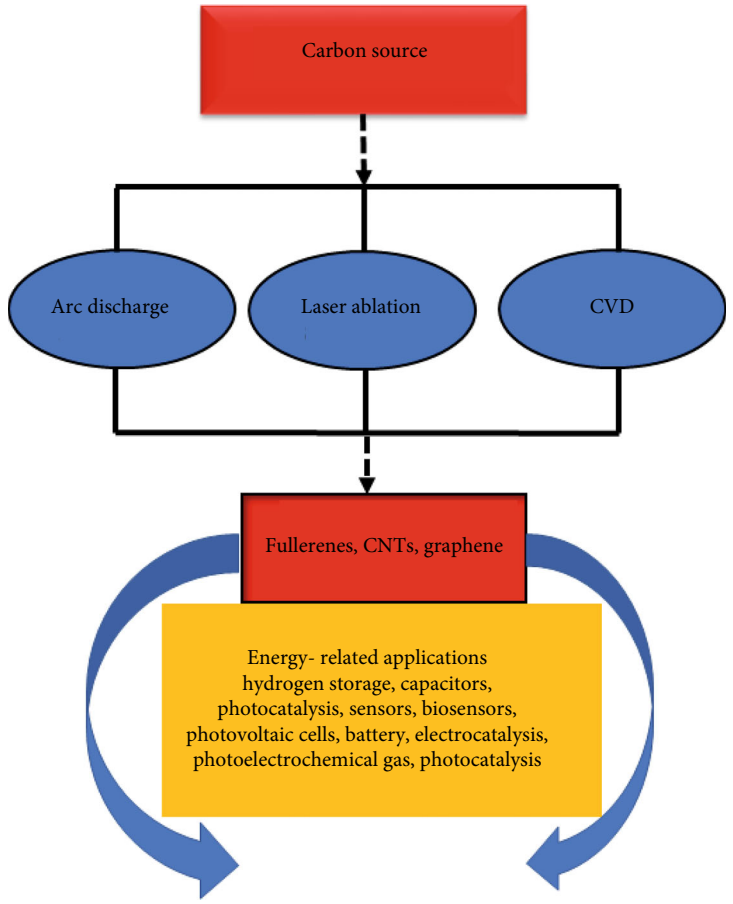

Figure 1: Graphical presentation of this study.

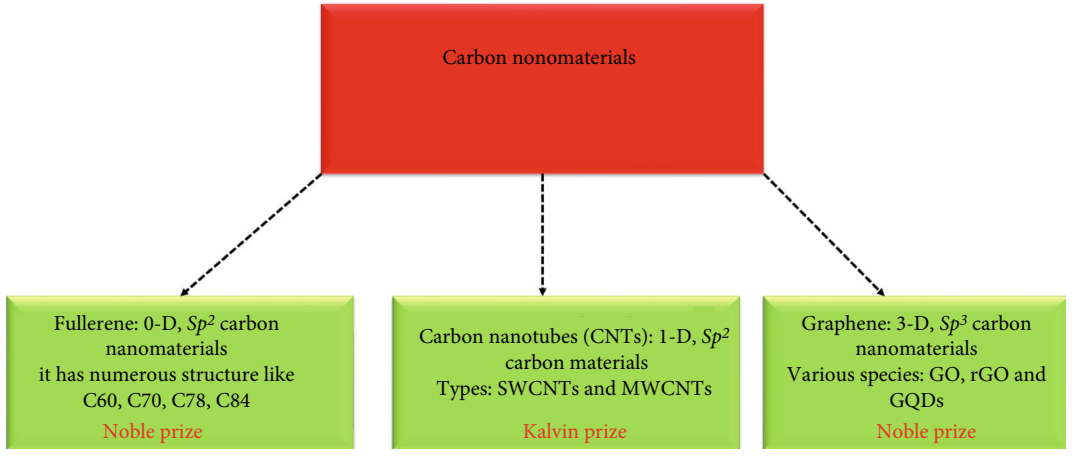

Figure 2: Carbon NMs (fullerene, CNTs, and graphene).

[16]. As shown in Figure 3, the C_{60} has spherical geodesic geometry with 12 pentagons and 20 hexagons rings. The 60 vertices are covered with 60 atoms of carbon and obey Euler's theorem

$$N - E + F = 2, \tag{1}$$

with N representing the quantity of vertices, E the quantity of edges, and F the number of faces. Euler's theorem indicates that irrespective of the vast number of cage hexagonal, each closed geometry must contain 12 pentagons to ensure a suitable curvature that will lock the cage [17]. Based on this theorem, the least fullerene that can occur is the unstable C_{20}. In the buckminsterfullerene molecule, each carbon particle is bonded covalently to the other three adjacent particles with sp^2 hybridization [15]. Furthermore, the existence

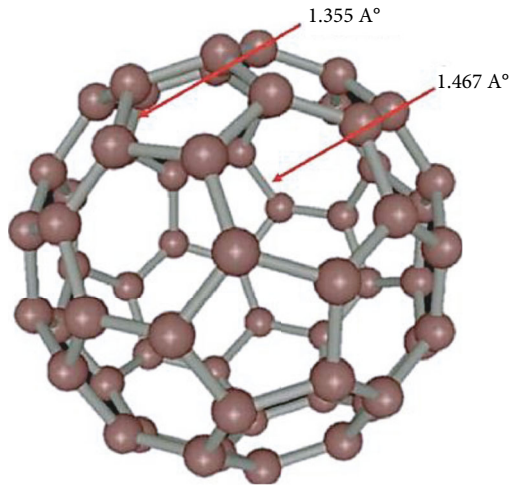

Figure 3: Structure of C_{60} [13].

of two bond lengths is apparent in fullerene (Figure 4) which is the C_5-C_5 single bond of 1.467 Å in the pentagons and the C_5C_6 double bond of 1.355 Å [13].

2.1.2. Species of Fullerene. Fullerenes can be modified chemically to exhibit various auspicious properties that are fundamental in their applications. For instance, an introduction of alkali metal to fullerene may result in a realization of superconductivity. Based on how these modifications are formed, four classes, namely alkali-doped, endohedral, exohedral, and heterofullerenes, are realized.

(i) Alkali-doped fullerenes: alkali-doped fullerides are the type of fullerenes class formed through a reaction of fullerene molecules and alkali metals. The reaction is a result of the high electronegativity of fullerene molecules which ensures the formation of compounds with atoms that can donate electrons. Examples are K_3C_{60} and Rb_3C_{60} alkali-doped superconducting fullerenes which have onset superconducting T_c of 18 K and 28 K, respectively [18].

(ii) Endohedral fullerenes: these are formed when an atom is trapped inside a hollow fullerene. If the atom closed inside is a metal, it leads to the formation of metallofullerene. Stable endohedral compounds are formed by metals such as yttrium, scandium, and lanthanum and some noble gases [19].

(iii) Exohedral fullerenes: these are a type of fullerene derivatives formed as a result of the reaction of fullerene and other chemical groups. Importantly, fullerene consists of conjugate $\pi-$system of the electron; it is expected that two main chemical transformations are likely to occur on the fullerene surface, further reaction leading to exohedral adducts and redox reaction leading to salts [20].

(iv) Heterofullerenes: it involves heteroanalogues of C_{60} and higher fullerenes. Here, an atom or more of carbon of the cage is/are replaced by heteroatoms like nitrogen and boron [21].

2.2. Carbon Nanotubes. The history of CNTs can be traced back to 1952 when it was first detected and theoretically described by Radushkevich and Lukyanovich [22]. Precisely, 24 years later, SWCNTs were reported during pyrolysis of a mixture of benzene and hydrogen [23]. The CNT discovery in recent times was ascribed by Iijima, who described MWCNTs in carbon soot produced during C_{60} carbon particle fabrication in an arc evaporation test [24].

The CNTs are 1-D nanomaterials with sp^3 hybridization of carbon atoms. Based on structure, CNTs can be grouped into two: SWCNTs and MWCNTs. The SWCNTs are formed when a graphene sheet is rolled up (Figures 5(a) and 5(b)), whereas the formation of MWCNTs involves several graphene coaxial tubes around the SWCNTs thus forming multiwalled CNTs. The simplest form of MWCNTs is double-walled CNTs (DWCNTs) formed by two sheets of graphene (Figure 5). Noteworthy, MWCNTs are either formed through the Russian Doll model or the Parchment model [26, 27].

The Russian Doll model explicates that MWCNTS are formed when CNTs of small diameter are enclosed by CNTs with a larger diameter whereas the Parchment model occurs when single graphene is rolled up around itself several times. Typically, the diameter of SWCNTs ranges from 0.40 to 2 nm and 1 to 3 nm for MWNCTs while the aspect ratios are higher than 1250 [5]. Other differences between SWCNTs and MWCNTs are enumerated in Table 1.

Geometrically, CNTs could be grouped into three: zigzag, armchair, and chiral as shown in Figure 6. The chiral vector $\vec{C}(n, m)$ in Figure 5(a) shows possible means of rolling up the honeycomb graphene. Mathematically, the chiral vector can be expressed as [1]

$$\vec{C} = (C_n = ma_1 + na_2). \tag{2}$$

By extension, the diameter of the tube can be determined as

$$d = \frac{a\sqrt{m^2 + mn + n^2}}{\pi}. \tag{3}$$

Here, $a = 1.42 \times \sqrt{3}$Å is the lattice constant in the graphite sheet. To determine whether the structure is armchair or zigzag, the following conditions must be met:

$$\theta = 0, (m, n) = (p, 0), \quad \text{where } p \text{ is interger (zigzag)}, \tag{4}$$

$$\theta = \pm 30^\circ\ (m, n) = (2p, -p) \text{ or } (p, p) \text{(airmchair)}, \tag{5}$$

where θ is the chiral angle formed between the chiral vector $\vec{C}$ and the zigzag direction and can be written as

$$\theta = \arctan\left[-\frac{\sqrt{3}n}{2m + n}\right]. \tag{6}$$

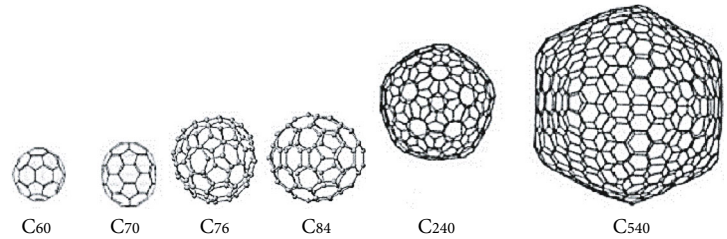

Figure 4: Illustrations of fullerenes (extracted from [12]).

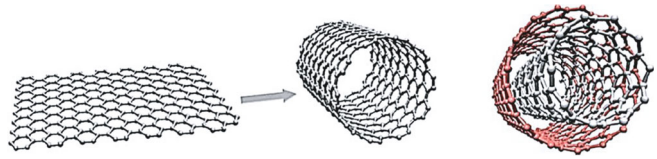

Figure 5: (a) Graphene sheet, (b) SWCNTs, and (c) DWCNTs [25].

Table 1: Differences between SWCNTs and MWCNTs [28].

SWCNTs	MWCNTs
Contain a monolayer of graphene	At least two layers of graphene
Requires catalyst during synthesis	Production could be done in the absence of a catalyst
Bulk synthesis is cumbersome	Easy bulk synthesis
A lot of defects during functionalization	Slighter defects occur during functionalization but are difficult to recover
Poor purity	High purity
Accumulates less in body	Accumulates more in the body
It is easy to characterize and analyse	Difficult to characterize and analyse
Twisting is easy	Twisting is difficult

Chirality is the most fundamental intrinsic property of the CNTs that have the greatest influence on optical and electronic properties. Most importantly, a small change of θ might transform a bandgap of CNT material resulting in a conductor or semiconductor (small or large bandgap semiconductor). There are two scenarios experienced in electronic applications; when $n - m = 3j$ (j is an integer), SWCNTs are metallic, whereas when $n - m = 3j +$ or $n - m = 3j + 2$, the SWCNTs are semiconductors. Metallic and semiconducting SWCNTs can be used as conducting wires and as channel materials in transistors, respectively [29]. Furthermore, CNTs could be utilized in quite several applications thanks to their excellent chemical and physical properties shown in Table 2

2.3. Graphene. Graphene is a single-atom-thick planar sheet of sp^2 covalently bonded carbon atoms in a honeycomb crystal lattice and the neighbouring atoms of carbon hexagons separated by a bond length of 1.42 Å and layer thickness of 3.3 Å (Figure 7) [30, 31].

Basically, three of the four valence electrons are allowed to bond to their next neighbours (σ-bonds), and the fourth electron (π-electron) is free (delocalized) and oriented perpendicularly to the sheet as shown in Figure 8(a). Again, graphene has crystal symmetry emanating from two sublattices that are equivalent. The energy bands of the sublattices intersect at zero energy, $E = 0$ (Figure 8(b)) thus leading to semimetal material [31].

Graphene acts as a building block for other carbon materials such as fullerene, CNTs and graphite. In addition to the excellent electrical conductivity, the great optical transmittance of about 97.7%, and the capability to withstand a current density of 108 A/cm^2, graphene material exhibits other exceptional properties as highlighted in Table 3. Due to the exciting properties, the study of graphene and its derivatives has attracted great attention in the recent past with numerous applications such as nanoelectronics, drug-agent delivery, electrodes, batteries, sensors, and supercapacitors [32].

2.3.1. Graphene Derivatives

(1) Graphene Oxide (GO). GO exhibits a hexagonal carbon structure that is comparable to that of graphene. However, it encompasses oxygen functionalities like carbonyl (C = O), hydroxyl (−OH), carboxylic acid (−COOH), and alkoxy (C − O − C) among other groups [39]. The oxygenated groups are responsible for the expansion of separation

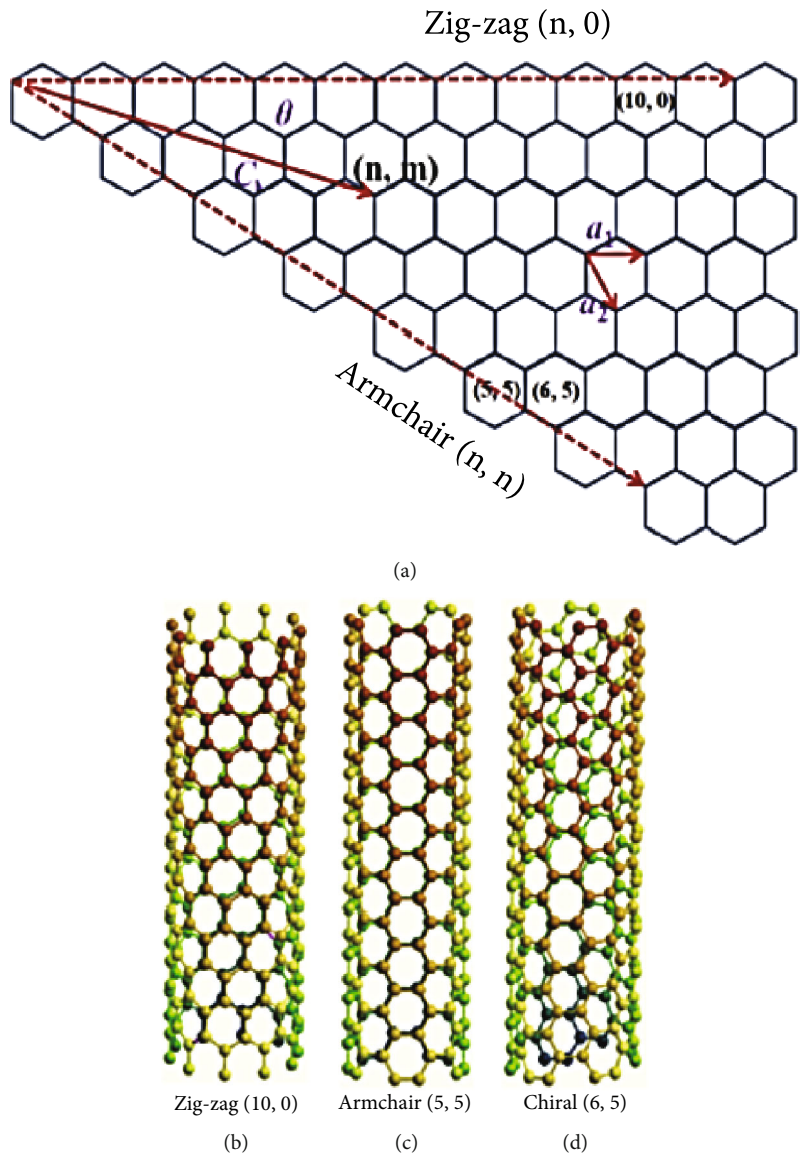

Figure 6: (a) Unrolled sole-layer graphene sheet showing the geometry of SWCNT, and (b–d) examples of the three categories of CNT sidewall, zigzag, armchair, and chiral version [29].

between the layers, increase of solubility, and provide the possibility for surface functionalization thus making it possible for use in nanocomposite (NC) materials.

High yields of GO can be synthesized/produced from graphite (Figure 9) as a raw material via chemical techniques that are less cost-effective. Also, its hydrophilic characteristic implies it can form aqueous colloids resulting in easy and cheap chemical processes. The GO sheets are composed of partly carbon atoms that are arranged tetrahedrally with sp^3 hybridization and displaced slightly on either side of the graphene plane [40]. These sheets are atomically rough because of the covalently bonded functional groups and the deformed structure [41].

(2) Reduced Graphene Oxide (rGO). Treatment of GO by various reducing synthesis methods results in the formation of reduced graphene oxide (rGO). In the literature, rGO is often known as functionalized graphene, chemically improved graphene, chemically transformed graphene, or condensed graphene [42]. The reduction of GO is aimed at improving the honeycomb hexagonal lattice which is otherwise distorted during oxidation from graphene to GO. Again, reduction ensures the minimization of oxygen groups and enhancement of properties that mirror pristine graphene [39].

(3) Graphene Quantum Dots (GQDs). On the other hand, GQDs are zero-dimensional (0-D), nanometer-sized carbon materials displaying features that are gotten from both graphene and carbon dots (CD). A conversion of 2-D graphene into 0-D GQD leads to an exhibition of innovative phenomena owing to the quantum incarceration and edge effects. These materials portray excellent photostability, biocompatibility, and low toxicity [43].

Table 2: Comparison of chemical and physical properties of SWCNTs and MWCNTs [5].

Chemical and physical properties	SWCNTs	MWCNTs
Strength	50.00-5.00 × 10^2GPa	10.00-60.00 GPa
Specific gravity	0.80 gcm^{-3}	1.80 g/cm^{-3}
Thermal conductivity	3.00 × 10^3Wm^{-1}K^{-1}	3.00 × 10^3Wm^{-1}K^{-1}
Specific surface area	4.00 × 10^2-9.00 × 10^2m^{2}g^{-1}	~ 2.00 × 10^2-4.00 × 10^2m^{2}g^{-1}
Thermal stability	2.80 × 10^4°C (in vacuum) >7.00 × 10^2°C (in air)	2.80 × 10^4°C (in vacuum) >7.00 × 10^2°C (in air)
Resistivity	5.00-50.00 $\mu\Omega$cm	5.00-50.00 $\mu\Omega$cm
Elastic modulus	~ 1.00 TPa	~ 0.30-1.00 TPa

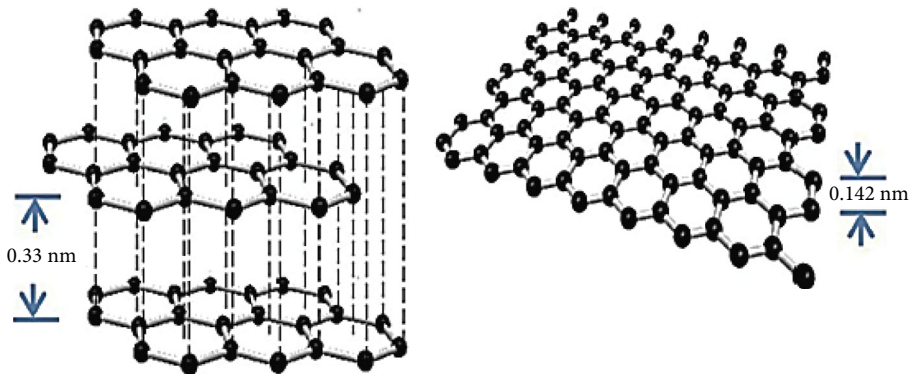

Figure 7: Representation of (a) graphite with layer separation of 0.33 nm and (b) graphene layer of thickness 0.142 nm [32].

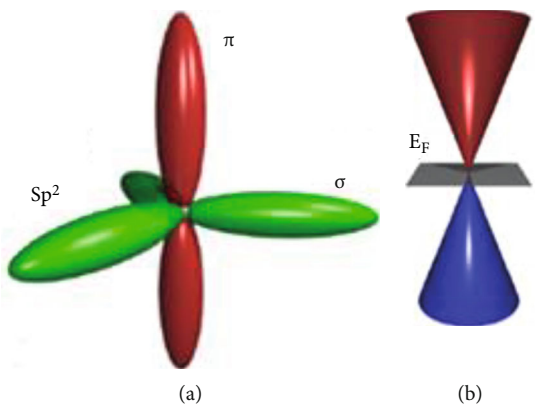

Figure 8: (a) Bonding of carbon atoms in graphene (b) schematic band structure at =0 [31].

3. Carbon Nanomaterial Synthesis

It is no doubt that carbon NMs have exciting properties which have guaranteed their usage in several applications. However, the implementation of these materials in wide-ranging applications has faced serious challenges due to structural inhomogeneity and imprecise fabrication emanating from the synthesis process. Nonetheless, many synthesis techniques have been developed together with continuous improvements of the existing methods which have not only seen the large quantity and high-quality production of carbon-based NMs but also saving of time and energy. For example, fullerenes have been synthesized via CVD [45], arc discharge, and laser ablation [5]. Equally, CNTs have been produced through arc discharge [46], laser ablation [47], CVD [48], solid-state pyrolysis [49] plasma torch, and liquid electrolysis [5]. In the synthesis of graphene, techniques such as exfoliation [50], chemical vapor deposition (CVD) [51], arc discharge [52], laser ablation (pulsed laser deposition) [53], unzipping of CNTs [54], Hummer's method [55], and chemical-based techniques [56] have been used. This section provides a detailed account of the three commonly used synthesis techniques: the arc discharge, laser ablation, and CVD.

Table 3: Physical and chemical properties of graphene.

Chemical & physical properties of graphene	Values	References
High thermal conductivity	5.00×10^3W m^{-1}K^{-1}	[33]
Carrier mobility	2.00×10^5cm^{2}V^{-1}s^{-1}	[34]
Electrical conductivity (σ)	2.00×10^3S.m^{-1}	[35]
Transparency	97.70%	[36]
Young modulus	1.00 TPa	[37]
Specific surface area	2.63×10^3m^{2}g^{-1}	[38]

3.1. Arc Discharge. There has been extensive use of the arc discharge technique to synthesize carbon NMs since its invention [14]. Importantly, the technique has undergone various modifications aimed at achieving specified objectives. The modifications include the usage of DC power in place of AC power, use of relatively low AC current compared to high AC current, the high practice of demineralized coal electrodes, and tapered apparatus for carbon soot collection [57]. As shown in Figure 10, the technique is an easy assembly with the possibility of giving relatively high yields and uses high purity graphite electrodes (anode and cathode). In a nutshell, depending on the nature of NMs desired, graphite anode is coated with a metal catalyst. The opening between the anode and cathode is regulated/controlled by regulating the anode position. During synthesis, high temperatures (above 17000°C) coupled with low pressures of 30-130 Torr and an inert gas-atmosphere are maintained with reaction time ranging from 0.50-1.00 minutes to 2.00-10.00 minutes [58]. It is worth noting that physical and chemical factors like reactor temperature, catalyst composition, the pressure of the gas (hydrogen), and carbon vapor concentration affect the arc discharge process.

During the synthesis of CNTs, several products are witnessed [58] in various sections of the reactor which include the following:

(i) Large quantities of soot are deposited at the reactor walls

(ii) Between the cathode and chamber walls, web-like structures are formed

(iii) At the end of the cathode, there is grey hard deposit

(iv) Around the cathodic deposit is a formation of spongy collaret

In the absence of catalysts, soot and deposit are the only products formed. It is imperative to note that the soot contains fullerene, whereas the carbon deposit comprises of MWNTs and graphite carbon NMs. The specifications of MWNTs formed are as follows: an inner diameter in the range 1.00-3.00 nm, an outer diameter between 2.00 and 25.00 nm, tube diameter $\leq 1\,\mu$m, and all having closed tips [58]. On the production of SWNTs, a catalyst of metals like Gd, Co, Ni, Fe, Ag, Pt, Pd, or mixtures of Co, Ni, and Fe with other elements like Co-Pt, Co-Ru, Ni-Y, Fe-Ni, Co-Ni, Co-Cu, Ni-Cu, Fe-No, Ni-Ti, and Ni-Y is used [59]. The outcome of this synthesis process includes the deposited core which is comprised of MWNTs, metal-filled FMWNTs, graphitic carbon nanoparticles (GNP), metal-filled graphite carbon nanoparticles (FGNP), and metal nanoparticles (NNP) and the spongy soot which includes MWNTS, FMWNTs, and SWNTs. This method produces relatively large quantities of CNTs, but chirality is compromised due to little control of alignment and requires purification to essentially remove traces of metallic catalyst [58].

Fullerenes were first synthesized using the arc method whereby carbon soot was produced through heating resistive graphite rods at a temperature of about 2.00×10^3°C and pressure of 100-200 Torr of either helium or argon gas [60]. More recently, a comparison of resistive heating of graphite and direct heating arc technique using a current of 150.00 A, pressure of 2.00×10^2 Torr, and 2 min arc discharge run produced a higher yield of about 67% of fullerene was obtained via resistive method compared to direct heating arc method [57].

Similarly, arc discharge has been used to fabricate graphene as attested by the SEM images of graphene (Figure 11) produced under 150 A and 200 Torr conditions [57]. Note that the nature/type of graphene produced is largely dependent on the environmental synthesis conditions. For example, Rao et al. produced a graphene sheet that consisted of 2-4 layers under the helium-hydrogen mixture. Also, the discharge atmosphere dictates the kind of bonds formed in as-produced graphene which ultimately influences the properties they exhibit. For instance, an atmosphere of H_2 and NH_3-B_2H_3 mixture resulted in the formation of B-doped graphene [61], whereas when H_2 and NH_3 atmosphere was used, N-doped graphene is achieved [62].

3.2. The Laser Ablation. The laser ablation technique (Figure 12) was first used by Guo et al. [63] and later developed and improved by other researchers [64, 65]. Unlike arc discharge, laser ablation works at significantly lower temperatures and uses solid carbon sources. Based on Geo et al.'s study [63], the set-up involves metal-graphite placed in a furnace which is heated to 1.20×10^3°C and bombarded by a laser beam of 532 nm. Under computer control, a smooth laser beam scanning is performed to ensure uniformity in vaporization. Subsequently, through laser vaporization, a production of soot is produced and then swept by argon gas from high temperature to a lower cooling collector (water-cooled copper) placed outside the furnace. The technique offers an easy one-step process in the production of carbon NMs such as graphene [66], diamond [67], carbon quantum dots [68], and carbon nanoparticles [69].

To synthesize the aforementioned carbon NMs, important laser ablation parameters like the wavelength of the beam, duration of the pulse, laser intensity, pressure flow type, between target and substrate, target and carrier-gas temperature are paramount. The technique guarantees potentially high yields and significantly low metallic impurities. Conversely, nanotubes produced by this method are not

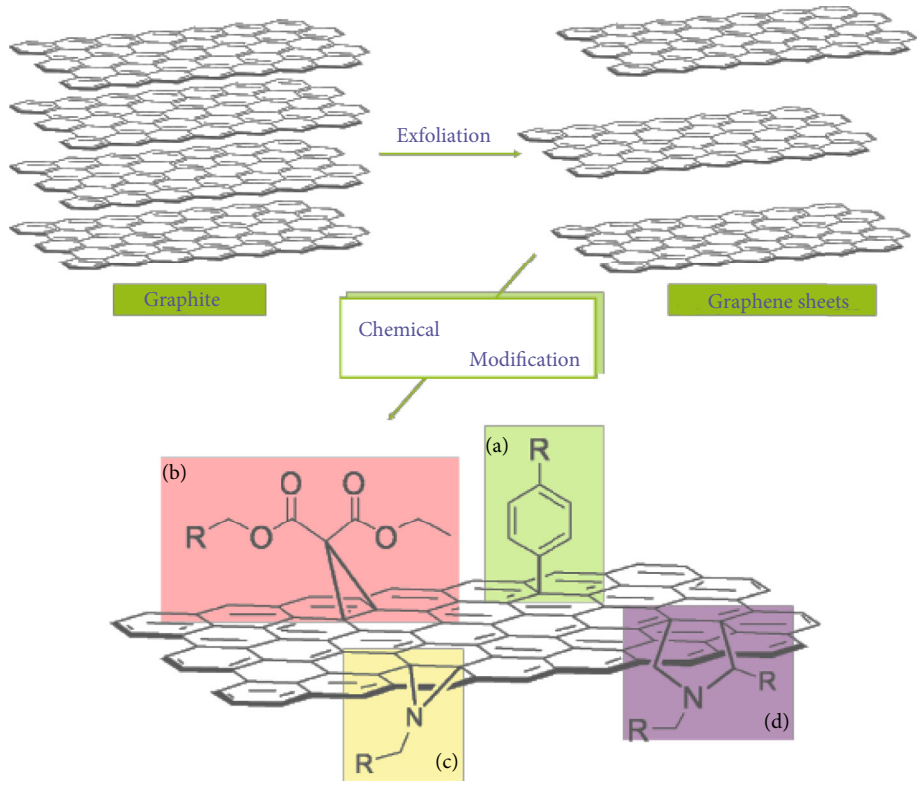

FIGURE 9: General chemical variation paths for exfoliated graphene sheets. (a) [3 + 2] 1,3-dipolar cycloaddition of in situ generated azomethine ylides. (b) [1 + 2] Bingel cycloaddition, (c) aryl diazonium, and (d) azide addition [44].

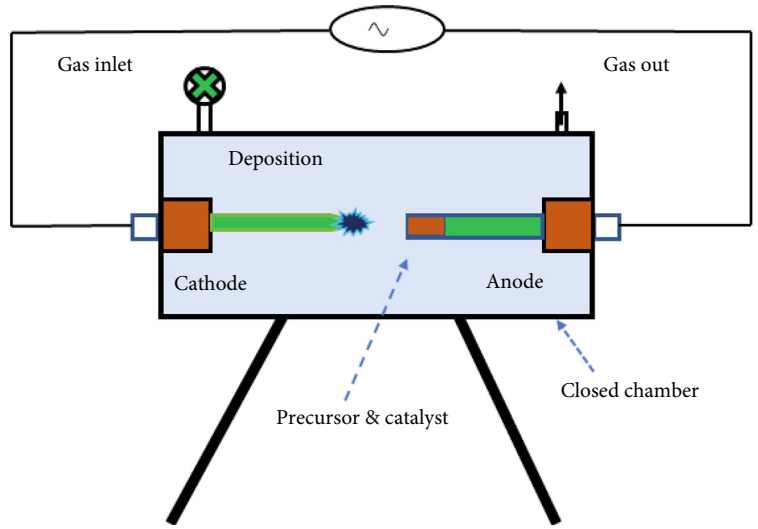

FIGURE 10: Arc discharge synthesis method.

essentially straight but have a degree of branching. Equally, their diameter is dependent on laser power. For example, in the absence of additional heating and by use of a continuous wave CO_2 laser ablation, an increase in the CO_2 laser power resulted in the production of SWCNTs with enhanced average diameter [25]. Also, the production is dependent on the wavelength and laser radiation fluence. It has been reported that with the use of 355 nm laser wavelength at fluence $F = 3$ J cm^{-2} produced good quality SWCNTs (Figure 13) were produced whereas for 1064 nm, good quality SWCNTs were obtained in the fluence range of $1 \leq F \leq 6$ J cm^{-2} but with lower yields for $F > 3$ J cm^{-2} [70].

A successful application of commercial MWCNTs and MWNTs-polystyrene targets (PSNTs) for the deposition of multifaceted thin films onto silicon substrates utilizing pulsed laser deposition (PLD) with pulsed, diode-pumped,

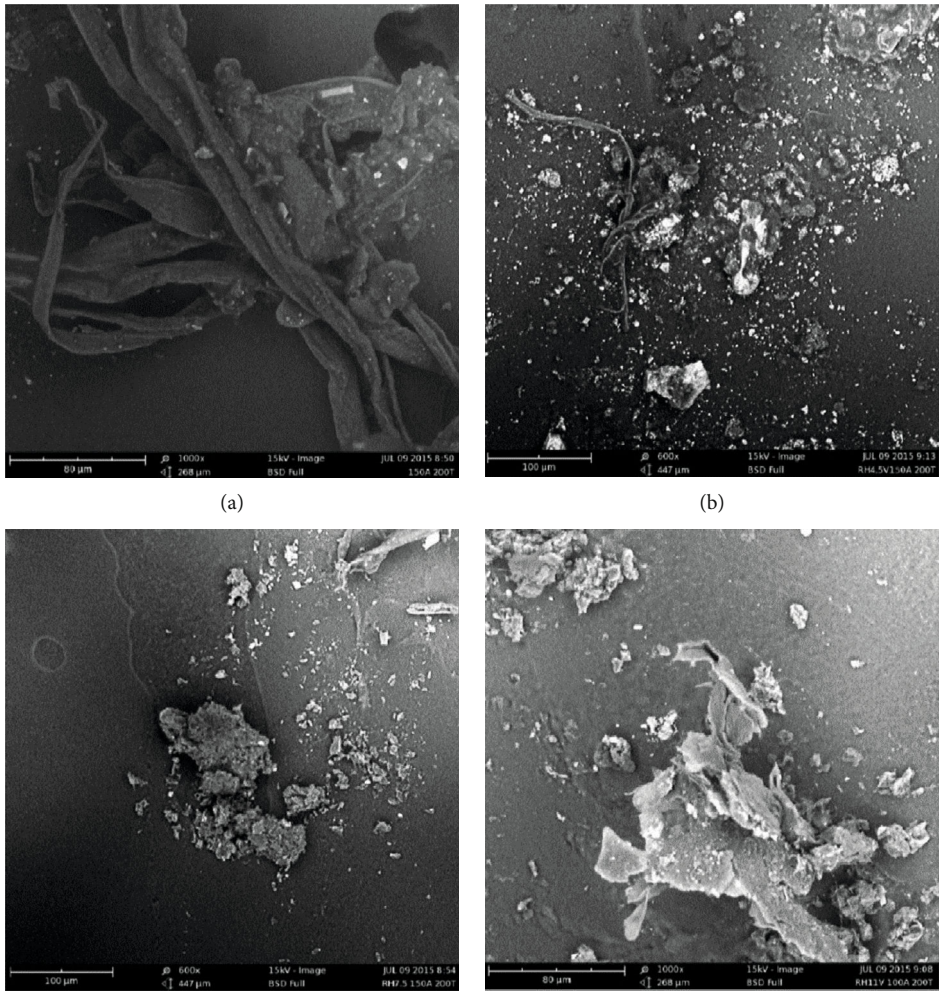

Figure 11: SEM images of graphene produced by arc discharge operating at 150.00 A and 200.00 Torr. (a) No resistive heating. (b) 4.50 V. (c) 7.50 V. (d) 11.00 V [57].

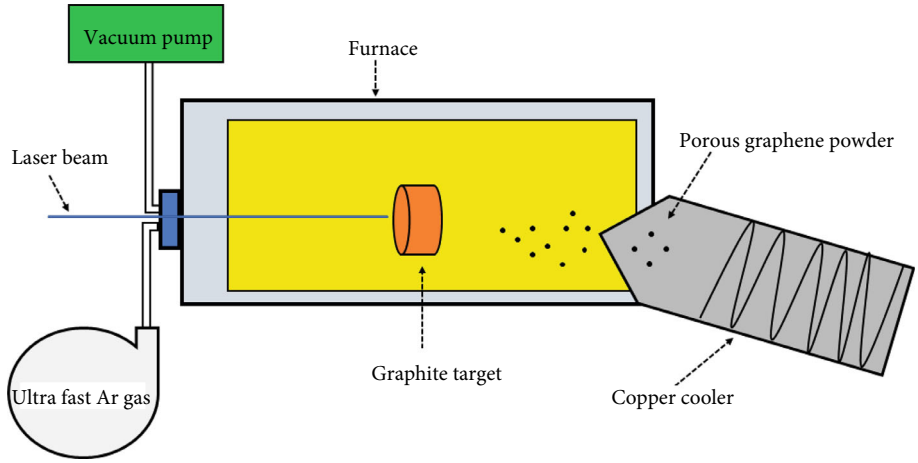

Figure 12: Schematic representation of laser ablation.

Tm : Ho : Lulf laser has been reported by Stramel et al. [71]. It has been observed that a thin film consisting of much higher quality is realized when using MWCNTs targets compared to PSNTs. Furthermore, using Nd : YAg laser, Bonaccorso et al. [72] prepared thin films of MWCNTs deposited by pulsed laser deposition on alumina substrates.

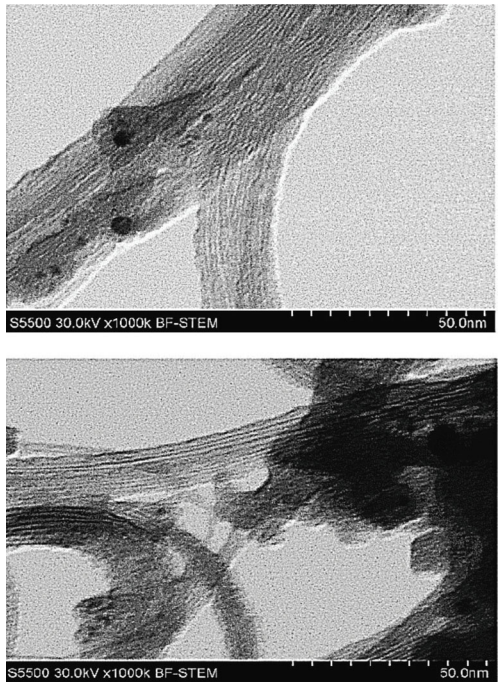

Figure 13: BF-STEM images of SWCNTs bundles. The metal NPs which act as a catalyst are shown by black dots [70].

Russo et al. [73] used an exceedingly oriented pyrolytic graphite (HOPG) as a carbon source in the synthesis of graphene. By employing this powerful technique, graphene is produced in a one-step process of exfoliating graphite sheets. The production process is conducted in a vacuum environment and under an inert gas atmosphere. Similarly, few-layered graphene (FLG) has been produced using femtosecond laser ablation of graphite powder suspended in ethanol. Interestingly, the setup does not require a controlled environment. The graphite powder used here was of an average size of less than 20.00 μm. Using a femtosecond laser of a wavelength of around 8.00×10^2nm and a beam diameter of around 8 nm, the powder was ablated and ultrasonication resulted in a formation of FLG of $\sim 1.00\,\mu$m in lateral size [74].

3.3. Chemical Vapor Deposition. CVD involves the disintegration of hydrocarbon or carbon monoxide feedstock with metal-catalytic help. Noteworthy, methane, ethylene, polycyclic aromatic hydrocarbons, and benzene are the main source of carbon used in CVD. This technique is performed in two configurations: horizontal furnace configuration and vertical furnace configuration. Being the most popular, we will discuss the horizontal configuration (Figure 14) as applied in CNT synthesis and which is typically similar to other allotropies of carbon NMs. The synthesis process begins with the placing of catalyst on ceramic or quartz boat/crucibles and then inserted into the quartz tube. At temperatures of between $5.00 \times 10^{2\circ}$C and $1.10 \times 10^{4\circ}$C, the reaction mixture comprised of inert gas and hydrocarbon which passed through the catalyst bed. This is followed by cooling of the system to room temperature [58]. Importantly, many different types of CVD have been developed that include hot filament (HFCVD), radio-frequency CVD (RF-CVD), microwave plasma (MPECVD), water-assisted CVD, oxygen-assisted CVD, and thermal or plasma (PE) oxygen assisted-catalytic chemical deposition (CCVD) [59].

Likened with the arc discharge and laser ablation, CVD is the most suitable technique for large scale production of CNTs given that it involves a simpler device and needs slighter situations in terms of temperature and pressure. Additionally, it is advantageous since control over diameter, wall number, length, and diameter are achievable thus capable of producing CNTs with desired morphology and structure. Imperatively, unless metal-catalyst is required to be removed, no purification is needed in this process. The role of catalysts in the production of CNTs is critical. Often, CVD system uses transition metal-based nanoparticle (NP) catalysts such as Co, Ni, Fe, Mo, ferrocene, and iron pentacarbonyl whose size correlates with the diameter of CNTs produced, i.e., a diameter of 0.5-5 nm for SWCNTs and 8-10 for MWCNTs [30].

Lehman et al. synthesized MWCNTs by employing hot-wire CVD (HWCVD) technique. The MWCNTs were grown on a lithium niobite ($LiNiO_3$) pyroelectric detector, heated at 600°C of temperature, with a pressure of 150 Torr and using nickel film as a catalyst [75]. Also, Dikonimos et al. [76] used H_2 and CH_4 as gas precursors to grow CNTs on nickel catalyst by a hot filament CVD (HFCVD) method with a temperature of about $1.80 \times 10^{3\circ}$C use of SiO_2 as substrate. Alternatively, CNTs were grown on Ni-coated Si substrates via MWCVD with H_2 and CH_4 gas and temperature between 5.20×10^2 and $7.00 \times 10^{2\circ}$C. The study showed a correlation between the size of Ni grains and Si substrates on the diameter of CNTs [77]. Likewise, using oxygen-assisted CVD, Byon et al. [78] synthesized SWCNTs using cobalt (Co) nanoparticles. The quartz tube was heated to a temperature of $9.00 \times 10^{2\circ}$C, and gases like H_2, CH_2, and C_2H_2 were introduced into the chamber. Oxygen flow was used at high temperatures to eliminate unreacted catalysts and amorphous carbon from the substrate. It was revealed that using the oxygen-assisted CVD method, high purity SWCNTs devoid of severe defects can be produced.

Kleckley et al. [79] designed an HFCVD and microwave improved CVD (MWCVD) technique to synthesize fullerene. In the case of HF-CVD, it was designed to have a filament current range of 50 A to 60 A and a temperature range of 2000-2200°C with stainless steel used as a substrate to hold thin film deposition. Essentially, for the development of CVD diamond thin films, the substrate temperature was between $9.50 \times 10^{2\circ}$C and $1.00 \times 10^{3\circ}$C feed H_2 of 99.99% purity and NH_4 of 99.80% purity with a controlled chamber pressure of between 30-100 Torr. On the other hand, the MWCVD method used a 100 W and 2.45 G generator as the excitation source and a quartz tube as the reaction chamber. They used Ar, H_2, and C_2H_2 gases and a pressure range of 1-10 Torr. The following observation was outlined: when $p > 25$ Torr, conducting film was formed inside a quartz tube with deposition taking a few minutes while at $p < 10$ Torr; a film deposition which was yellow in colour was observed inside the walls of the quartz tube. This colour was transformed to dark brown on exposure to plasm for 30 min.

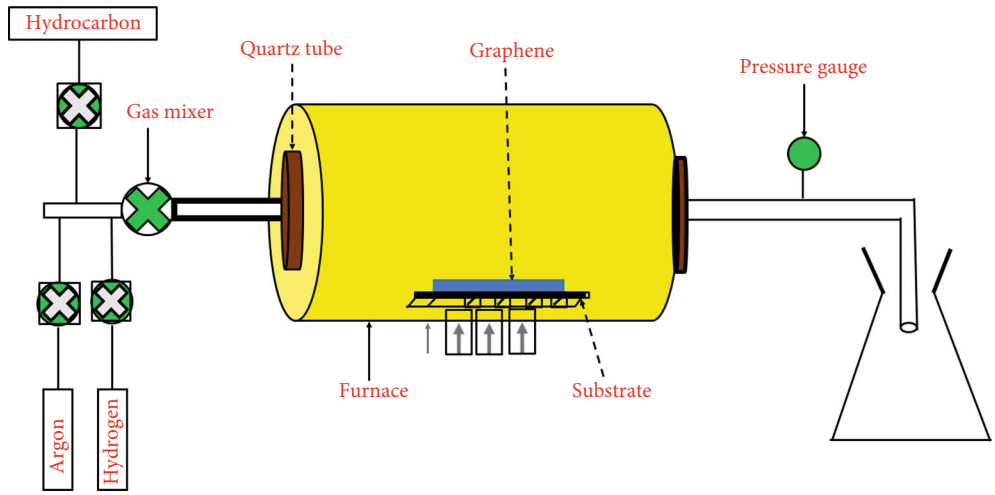

Figure 14: Sketch of CVD synthesis technique.

Kang et al. [80] synthesized fullerene-intercalated pCNFs utilizing a Fe/Y catalyst on a Cu substrate. Fullerenes were inserted in the graphitic interlayer spacing as an alternative to attaching them to the surface of the CNFs. The incorporation of yttrium oxide in the composite is supposed to play a critical role in the formation of fullerene by CVD. Also, nanoonion-like fullerene (NOLFs) has been synthesized by catalytic deposition of acetylene. The temperature of $4.20 \times 10^{2^\circ}$C was used, and Fe supported on NaCl acted as a catalyst. The catalyst consisted of 0.30, 1.60, 3.30, and 5.20 wt.% of Fe. The NOLFs formed had a structure of slanted graphitic fragments whose diameter ranged between 15.00 and 50.00 nm. Imperative to note that at a temperature of $1.10 \times 10^{4^\circ}$C in the vacuum, a clear concentric graphitic NOFLs was produced [81].

For the synthesis of graphene, precursors are characteristically adsorbed on the crystalline substrate surface which is then decomposed at relatively high temperatures and inert atmosphere. This generates sites of adsorption on the substrate which results in the generation/development of uniform thin films. Production of graphene on a clean surface improves graphene quality since this minimizes structural defects and ensures uniform nucleation. Based on various industrial applications, the CVD synthesis of graphene has been proved to be cost-effective, reliable, and feasible [7]. Similar to CNTs, catalysts such as Pt, Ni, Ru, Co, and Cu play a vital role during graphene synthesis. For instance, reports show a synthesis of sole-layer graphene to few-layer graphene films using Ni substrate when hydrocarbons such as methane, ethylene, and camphor are heated at temperatures of about $7.00 \times 10^2 - 8.50 \times 10^{2^\circ}$C and argon used as a carrier gas [82, 83].

Similarly, the CVD process has been employed in the synthesis of large-scale graphene films. High growth temperature of the range 900-1000°C was used in the self-heat catalytic metal layers of the SiO_2/Si. It was shown that the method produced high-quality films whose electrical and structural properties are compared well with those produced via hot-wall CVD [84]. In addition, radiofrequency plasma-enhanced CVD (RF-PECVD), which is a very cost-effective technique in the synthesis of high-quality graphene, was reported by [85]. Here, SiO_2 substrates covered with Ni thin film are used together with low temperatures of 650°C. Then, an introduction of CH_4 into the chamber is done which culminates in the deposition of sole-layer or few-layer of graphene on Ni film.

4. Applications of Carbon Nanomaterials

The advancement of nanotechnology in recent years has been nearly felt in all industrial sectors thanks to the discovery of novel NMs which possess exceptional properties. As NMs, carbon-based NMs have found exciting applications in the medical field (biosensing, drug delivery, tissue engineering, and therapy), energy (hydrogen storage, electrodes, photocatalysis, and photocells), environmental monitoring and remediation (sensing and removal of heavy metal and toxic gases), and electronics (thin films and transistors etc.) among many more (Figure 15). Ideally, the huge potential in these materials continues to attract attention in research, and any implementation in the new technology is expected to revolutionize human life. Here, we highlight, albeit briefly, energy-related research and applications of carbon-based NMs.

4.1. Applications of Fullerenes

4.1.1. Hydrogen Storage. The noble characteristic that presents fullerenes as the perfect storage system for hydrogen is the fact that C-C bonds can be hydrogenated resulting in the formation of C-H bonds. Worth noting, the C-H bonds have lower bond energies, and when subjected to heat, they are bound to break thus reverting to their distinctive fullerene structure. Ab initio approximations within density functional theory (DFT) have been broadly used to study carbon and boron fullerenes as possible hydrogen storage media [86–88]. For instance, Yoon et al. [86] conducted DFT studies in charged carbon fullerenes $C_n (20 \leq n \leq 82)$ systems. It

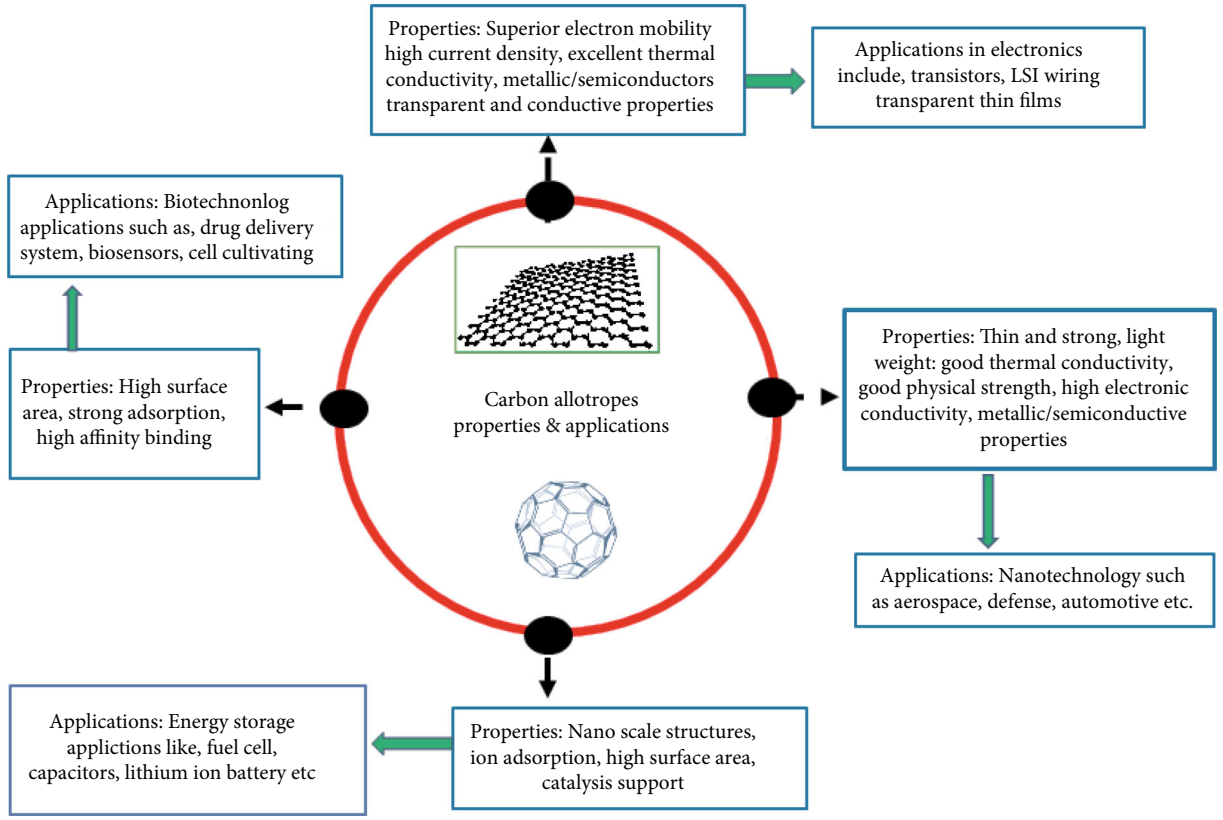

Figure 15: Carbon NM properties and possible applications.

was established that the binding strength of molecular hydrogen was greatly enhanced to 0.18-0.32 eV which is potentially suitable for room temperature-ambient applications with results revealing that up to ~8.00 wt.% of storage capacity can be achieved by the charged fullerene. Similarly, functionalizing C_{60} fullerene through coating with light alkaline-earth metals showed that Ca and Sr will strappingly bind to the C_{60} surface. Importantly, the binding is attributed to charge transfer mechanisms that involve the empty *d* levels of Ca and Sr metals. The charge redistribution produces electric fields which act as ideal hydrogen attractors, and the studies revealed that $Ca_{32}C_{60}$ had superior hydrogen uptake of >8.4 wt.% [87]. Also, the binding capability and hydrogen storage efficiency of Ti-decorated B_{40} fullerene have been investigated, and results show excellent binding ability compared to other transition metals. Also, 34 H_2 molecules can be stored by B_{40} fullerene layered with 6Ti atoms (Ti_6B_{40}) which corresponds to 8.70 wt.% [88].

4.1.2. Energy Materials. The usage of fullerene materials in energy-related materials and applications has considerably optimized material properties and enhanced operations. For example, they have been used in capacitors, lithium batteries, and the production of superconductivity.

(1) Capacitors. In supercapacitors, the capacitance of surface electrode is mostly influenced by pore size distribution, surface area, and accessibility of electrolyte and conductivity [89]. Research has shown that the use of hybrid NMs can provide excellent materials [90]. A composite system of fullerene and graphene (C_{60}/graphene) has been found to have a specific capacitance of about $1.35 \times 10^2 F\,g^{-1}$ at the current density of $1.00\,A\,g^{-1}$. This value is high when compared to $101.88\,F\,g^{-1}$ for pure graphene. Also, for the 1.00×10^3 charge/discharge cycle, the composite exhibited an amazing retention rate of 92.35% [91]. Also, a high specific capacitance of 8.13×10^2 Fg^{-1} at a current density of $1.00\,Ag^{-1}$ for a composite of C_{60} whisker (FW)/polyaniline emeraldine base (PANI-EB) compound has been reported. The composite exhibited low electrical resistance, and for 1.50×10^3 cycles, a rendition of 85.20% was witnessed which affirms the influence of the use of fullerene C_{60}[92].

(2) Lithium-Ion Anode and Cathode. The use of fullerene in lithium-based batteries guarantees safety and a longer life cycle. Studies have shown that an application of hydrogenated fullerenes as a high-performance anode results in a significant reduction of the irreversible capacity and improved the reversible capacity [93]. Density functional theory (DFT) studies of fluorine encapsulated $B_{12}N_{12}$-fullerene as anode for the lithium-ion battery showed that the pristine cluster has low electrochemical cell voltage V_{cell} of 1.09 V, but with encapsulation with fluorine, a significant increase of V_{cell} to 3.07 V was established [94]. Based on their high electron affinity, fullerenes can as well be used as cathodes. DFT studies on electrochemical properties of

boron-doped fullerene derivatives revealed a considerable rise in the redox potential from about 2.46 V to 3.71 V when boron-doped C_{60} was used as a cathode [95].

(3) Superconductivity. An emergence of superconductivity involving fullerene has been observed when an alkali metal is entrenched within the holes of the fullerene C_{60}. For example, cesium (CS), rubidium (Rb), and potassium (K) doping have resulted in the formation of superconductors $CS_xRb_yC_{60}$, RbxC$_6$, K_xC_{60}, and K_xC_{60} superconductors with T_c of 33 K, 29 K, and 18 K, respectively [96, 97]. Furthermore, a discovery of a hole-doped fullerene $C_{60}/CHBr_3$ with the highest $T_c = 117$ K among fullerene-based superconductor has been prepared under ambient pressure [98]. It is imperative to note that superconductors are well characterized by two phenomena, namely, the Meissner effect (exclusion of magnetic flux) and zero/negligible resistance. Therefore, the fact that superconductors can be formed from fullerenes is of great interest in the electronics industry.

4.2. Applications of CNTs

4.2.1. Photocatalysis. Photocatalysis is a catalytic acceleration of a photo-induced chemical process [99]. Semiconducting materials such as TiO_2, CdS, ZnO, CuO, and GaP play a critical and unmatched role in photocatalysis owing to their exceptional electronic band structure which is comprised of an empty conduction band and filled valence band. A combination of TiO_2 and CNTs has attracted considerable attention in photocatalysis where the functional mixtures and composites have been used for the photodegradation of acetone, benzene, azo dyes, phenol, and oxynitride [100]. The CNT-enhanced photocatalysis can be ascribed to the auspicious electronic features of CNTs with a report showing large electron-storage capacity [101]. For example, Shaban et al. synthesized TiO_2 nanoribbons (TiO_2 NRs) loaded with FeCo-Al_2O_3 catalyst and utilized it as a precursor for the fabrication of TiO_2 nanoribbons/CNTs (TiO_2 NRs/CNTs). Loading TiO_2 NRs by FeCO-Al_2O_3 catalysts under the CVD synthesis method produced TiO_2-B nanoribbons with a shifted band gap of 3.09 eV [102]. Similarly, Kamili et al. [103] synthesized various MWCNTs/titanium oxide NCs employing a low-temperature sol-gel technique and simple evaporation and drying procedure. They observed that the maximum ratio of BBR photodegradation was achieved with a composite having an MWCNT/TiO_2 ratio of 0.5% (w/w). Furthermore, MWCNT enhanced the photocatalytic activity of TiO_2. Also, the presence of MWCNT (0.50 wt.%) caused a decrease in the TiO_2 bandgap from 3.25 to 2.8 eV.

4.2.2. Photoelectrochemical Cells. A PEC, a photocurrent-generated component, is formed by an electrolyte and photoactive semiconductor electrode. Imperatively, the generation of electron-hole pairs is realized when the electrolyte-semiconductor interface is irradiated by an energy that is greater than the semiconductor bandgap. After it was discovered in 1970, the Honda-Fujishima effect of PEC water splitting on semiconductor constituents has gained immense attention in solar energy study. The PEC provides an effective and environmental-sustainable/friendly way of generating hydrogen from water utilizing solar energy [100]. The working principle of the PEC involves a working photoanode that engrosses light to oxidize water thus producing photo-excited electrons, oxygen gas, and protons. This is followed by a collection and transportation of the photo-induced electrons to a counter-cathodes that are achieved through the external circuit [100].

Kim et al. [104] fabricated PEC cells employing n-type TiO_2 as the anode- and metal-coated CNTs as a cathode. They observed that the PEC metal decorated CNTs cathode yielded a large photo-voltage compared to the Pt cathode owing to the p-type semiconducting possessions of CNTs. Also, the PEC produced a photo-voltage of approximately 1.35 V which is greater than the 1.23 V that is needed for water splitting.

Kim et al. [105] modified the Fe_2O_3 photoanode by graphene-CNTs compound conducting framework for the effective transfer of Fe_2O_3 constituent parts to transport conducting oxide substrate in PEC water splitting cells (Figure 16). Likened to the bare Fe_2O_3 photoanode at 1.23 V vs RHE, the Fe_2O_3 compound anode exhibited a photo-current rise of 530%. Similarly, a photo-current increase of 200% and 240% was observed in Fe_2O_3-CNT and Fe_2O_3-graphene photoanodes, respectively. They attributed the performance improvement by the composite framework to synergistic effects induced by the development of 3D-like structures from 1 D CNT and 2D graphene [105]. Furthermore, the gel-centrifugation method was used to prepare SWCNTs thin films containing a high density of semiconducting CNTs meant for PEC application. Importantly, results showed that photocurrent produced by semiconducting SWNTs film was higher compared to conventional unsorted SWNCTs films. This was a consequence of condensed recombination channels made possible by the elimination of metallic nanotubes [106].

4.2.3. Electrocatalysis. This is a study involving the relationship between electrode materials' physiochemical properties and the rate of the chemical process. Fundamentally, electrocatalysis is aimed at improving the reaction rate. In that regard, the production of efficient and cost-effective electrocatalysts has momentously improved technologies like batteries, fuel cells, artificial photosynthesis, biosensors, and CO_2 reductions [100].

The superior chemical and electrical properties of CNTs have guaranteed their use in these technologies. Lee et al. synthesized a variety of MWCNT-supported Pt NC by both the aqueous solution reduction of Pt salt and the decrease of Pt ion salt in ethylene glycol (EG) solution. For purposes of comparison, Pt/XC-72 NC too was synthesized through the EG method. It was established that all MWNCT-supported Pt catalysts exhibited enhanced oxygen reduction reaction (ORR) and greater cell performance compared to XC-72 supported catalysts [107]. Also, Yang et al. synthesized boron-doped CNTs (BCNTs) with tunable boron content of 0-2.24 atom % meant for fuel cell application. It was observed that the ORR inception and highest potentials positively shifted, and the current density was amplified with an

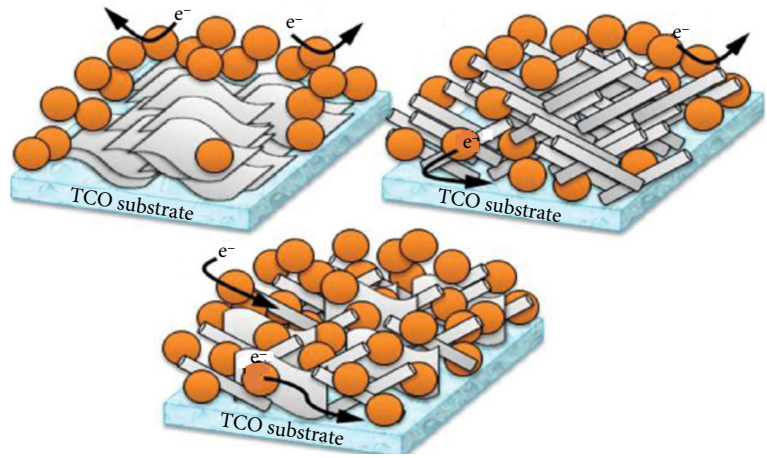

FIGURE 16: Iron oxide photoanodes improved with conducting frameworks of unadulterated graphene (A), CNT (B), and graphene-CNT compound (C) [105].

increase in boron content. This is an indication of a robust dependence of the ORR on boron content [108]. Furthermore, a replacement of noble metals by utilization of modified CNTs in fuel cells has increased momentum in the recent past. A breakthrough on this was realized when vertically aligned nitrogen-containing CNTs (VA-NCNTs) were fabricated. The study noted that VA-NCNTs possessed high electrolytic activity for ORR [109].

4.3. Applications of Graphene

4.3.1. Battery. Owing to the outstanding specific capacity and reversibility, graphite has been utilized in Li-ion batteries as an anode. However, demand for Li-ion batteries is on the rise and there is an urgent need for more production. The graphene-based anode has been touted as the most ideal carbonaceous candidate due to its superior electrical conductivity, σ, chemical tolerance and outstanding surface area [82]. Figure 17 shows a structure of SnO_2/GNs fabricated using SnO nanoparticles, graphene nanosheets and ethylene glycol. Measurements carried on the SnO_2/graphene showed an adjustable capacity of 8.10×10^2 mAh/g and an enhanced cycling performance [110]. Also, a self-assembled TiO_2-graphene hybrid nanostructure was fabricated by Wang et al. [111] and graphene stabilization in an aqueous solution which was made possible by the use of anionic surfactants was ensured during the fabrication. This also facilitated the self-assembly growth of TiO_2 with graphene. Importantly, a significant increase of specific capacity from 35.00 mAh/g in rutile TiO_2 to 87.00 mAh/g was detected.

Furthermore, it has been noted that the use of graphene enhances battery charging rate by allowing faster electron and ion transport in the electrodes. For example, Li et al. [112] fabricated a fast-charging lithium-ion battery by loading nanoscale $Li_4Ti_5O_{12}$ and $LiFePO_4$ cathode materials on graphene foam. The hybrid electrodes ensured the battery was fully charged in only 18 seconds.

4.3.2. Photovoltaic Cells. Graphene-based NMs have been extensively examined in photovoltaic technology owing to their excellent properties such as high carrier mobility, high mechanical strength, high optical transparency, and zero bandgaps. For instance, 0-D graphene quantum dots are exceptional fluorescent NMs with novel properties originating from their unusual quantum confinement and edge effects which play a significant role in the photoluminescence of GQDs [113].

Importantly, graphene and graphene derivatives are functionalized either during synthesis or during treatment to control and optimize surface properties. Quite several graphene-related photovoltaic cells such as dye-sensitized cells, organic bulk-heterojunction, hybrid ZnO/poly(3-hexylthiophene) (P_3HT), Si-based, and InGaN p-i-n have been reported [114].

For an application as conductive electrodes in organic photovoltaic cells, multilayer graphene (MLG) films were synthesized at diverse growth temperatures via the CVD method. Power conversion efficiency (PCE) of 1.3% was recorded in MLG films with 1000 C which was deemed the best. An enhancement of the PCE to 2.6% was made possible with an insertion of a hole-blocking TiO_x layer in the structure [115].

Liu et al. fabricated an organic photovoltaic cell founded on an acceptor of solution-processable functionalized graphene (P_3HT/graphene based solar cell). The structure was comprised of ITO/PEDOT : PSS/P3HT : graphene (indium tin oxide/poly(ethylene dioxythiophene)) doped with polystyrene sulfonic acid/poly(3-hexaylthiopene-1-3-diyl) : graphene. The device recorded a short current density (J_{SC}) of 4.0 mAcm^{-2}, PCE of 1.1%, and open-circuit voltage (V_{OC}) of 0.72 V [116]. Likewise, functionalized graphene devices with structural formation ITO/PEDOT : PSS/P_3HT : functionalized graphene/LiF/Al was designed. The best performance was observed in a device containing 10% of graphene with PCE of 0.88%, V_{OC} of 0.77 V, and J_{SC} of 3.72 mAcm^{-2}[117].

4.3.3. Sensors and Biosensors. The use of graphene-based sensors and biosensors in the detection of gases, chemical compounds, and biomolecules is well known [118–120]. For instance, the detection of gases (H_2O_2, H_2S, NO, NH_3, and CO_2), toxic hydrocarbons, heavy metals, and pharmaceutical pollutants have been made possible via these sensors as depicted in the schematic of Figure 18 [121]. The change of

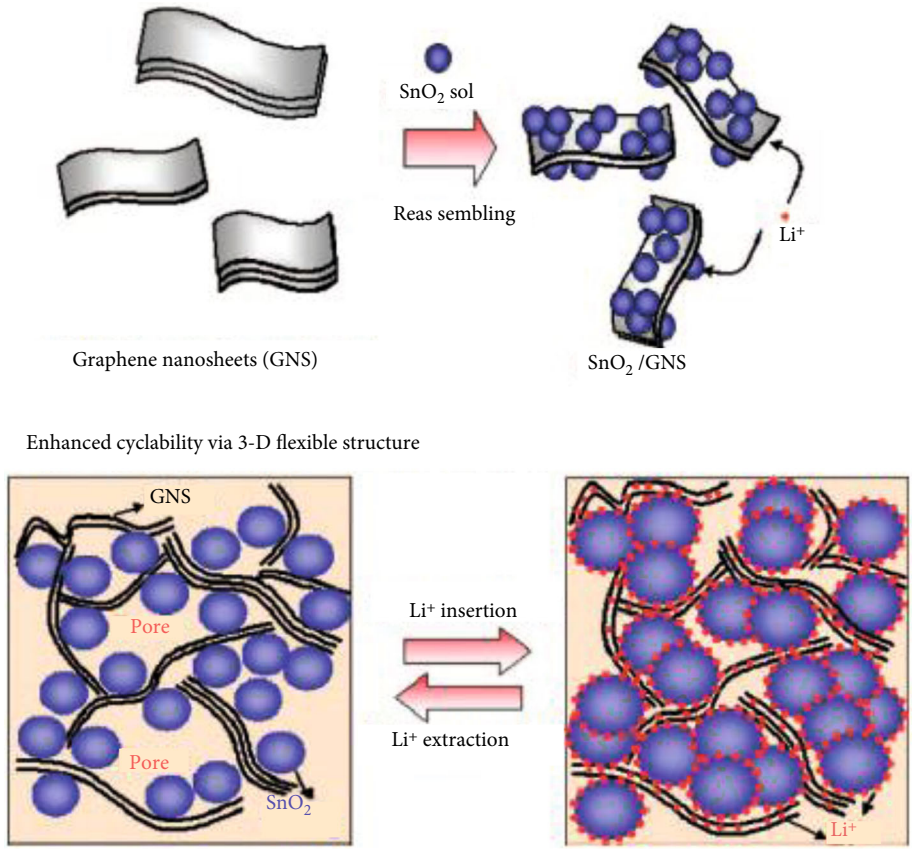

Figure 17: Illustration of the fabrication of SnO_2/GNS [110].

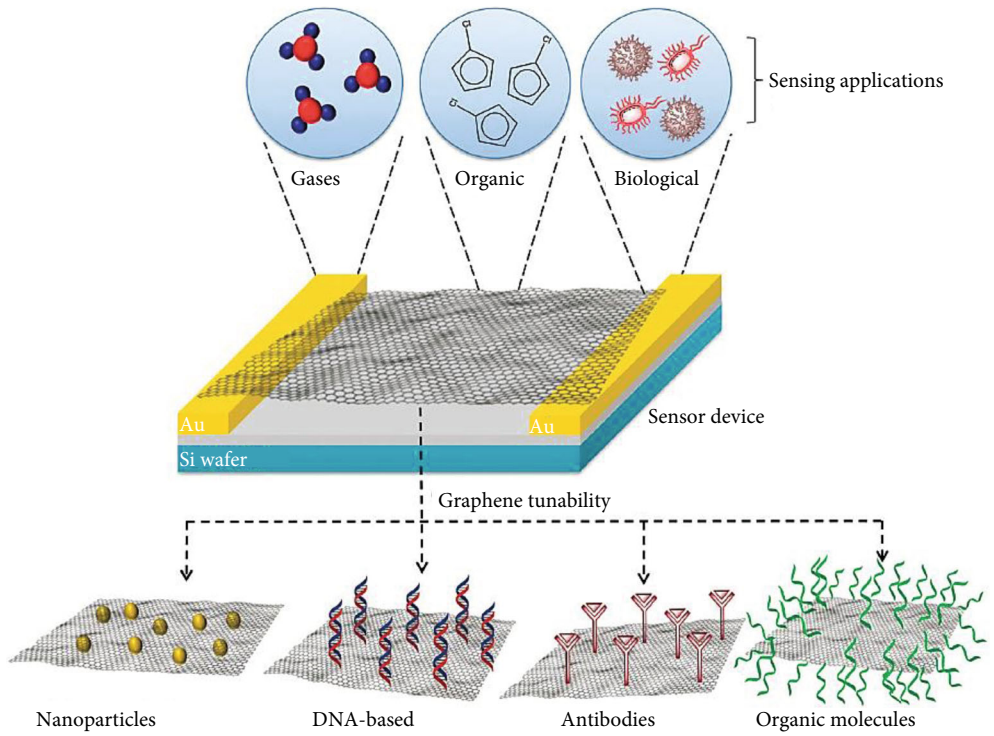

Figure 18: Graphene-based sensors for detection of organic molecules, gases, biomolecules, and microbial cells [121].

σ of graphene due to the adsorption of particles on graphene surface forms the basis of operational principles biosensors fabricated by graphene. Here, the change in σ is ascribed to carrier concentration change emanating from adsorbed gas molecules acting as donors or acceptors [37, 82].

Studies by Schedin et al. [122] reported excellent detection of NO_2, NH_3, H_2O, and CO_2 by graphene. The research study also demonstrated that holes and electron doping in high concentrations could hardly affect the movement of graphene. Also, studies by Fowler et al. [123] showed sensing of NO_2, NH_3, and dinitrotoluene (DNT). The mechanisms of sensing in NO_2 and NH_3 were attributed to hole-induced conduction and electron-induced conduction, respectively. The former happens when an electron is withdrawn from graphene while the latter is a result of the donation of an electron to graphene. The mechanisms of DNT detection were found to be similar to NO_2 sensing. On the other hand, research on glucose properties of graphene-biosensing using glucose oxidase (GOD) has been reported [124]. Here, a fabrication of polyvinylpyrrolidone protected graphene/polyethyleneimine functionalized ionic liquid/GOD electrochemical biosensor was developed. An electron transfer that was observed affirms the suitability of graphene in glucose sensor construction. A comparison of graphene based-glucose sensors to CNT-based sensor reveals that graphene sensors are more effective in the detection of catecholamine neurotransmitters (dopamine and serotonin) thus demonstrating the superiority of graphene [125, 126].

5. Conclusion and Future Perspectives

Presently, carbon NMs and their derivatives have received special attention. This can be attested by voluminous research work that covers this particular scintillating area. Their excellent properties such as optical, mechanical, chemical, and electrical are unmatched by any conventional material. However, there is a lack of macroscopic quantity production of these materials to match the industrial needs. Furthermore, structural nonhomogeneity and vague fabrication have hindered vigorous and consistent implementation of these materials in extensive technologies. That notwithstanding, we have highlighted some of their energy-related applications and the critical role they play in nanotechnology. We recommend that the future work perspectives ought to be anchored on the optimization of their properties, improvement of existing, and invention of synthesis techniques. Hence, more advanced research that will enhance the development of carbon NMs and their derivatives for various applications such as the ones reviewed in this study should be given the necessary attention.

Data Availability

Completely, data produced or investigated during this work were involved in this submitted article.

Conflicts of Interest

There is no conflict to declare.

Authors' Contributions

Kingsley Eghonghon Ukhurebor is the submitting author. All authors contributed significantly to this review study.

Acknowledgments

The authors are grateful to their respective institutions and authors whose publications were used for this review study.

References

[1] M. Terrones, "Science and technology of the twenty-first century: synthesis, properties, and applications of carbon nanotubes," *Annual Review of Materials Research*, vol. 33, no. 1, pp. 419–501, 2003.

[2] R. Onyancha, K. Ukhurebor, U. Aigbe et al., "A systematic review on the detection and monitoring of toxic gases using carbon nanotube-based biosensors," *Sensing and Bio-Sensing Research*, vol. 34, p. 100463, 2021.

[3] U. Aigbe and O. Osibote, "Carbon derived nanomaterials for the sorption of heavy metals from aqueous solution: a review," *Environmental Nanotechnology, Monitoring & Management*, vol. 16, p. 100578, 2021.

[4] D. Jariwala, V. Sangwan, L. Lauhon, T. Marks, and M. Hersam, "Carbon nanomaterials for electronics, optoelectronics, photovoltaics, and sensing," *Chemical Society Reviews*, vol. 42, no. 7, pp. 2824–2860, 2013.

[5] R. Onyancha, U. Aigbe, K. Ukhurebor, and P. Muchiri, "Facile synthesis and applications of carbon nanotubes in heavy-metal remediation and biomedical fields: a comprehensive review," *Journal of Molecular Structure*, vol. 1238, p. 130462, 2021.

[6] Y. Manawi, A. Samara, T. Al-Ansari, and M. Atieh, "A review of carbon nanomaterials' synthesis via the chemical vapor deposition (CVD) method," *Materials*, vol. 11, no. 5, p. 822, 2018.

[7] E. Agudosi, E. Abdullah, A. Numan, N. Mubarak, M. Khalid, and N. Omar, "A review of the graphene synthesis routes and its applications in electrochemical energy storage," *Critical Reviews in Solid State and Materials Sciences*, vol. 45, no. 5, pp. 339–377, 2020.

[8] E. Osawa, "Superaromaticity," *Kagaku*, vol. 25, pp. 854–863, 1970.

[9] H. Kroto, J. Heath, S. O'Brien, R. Curl, and R. Smalley, "C_{60}: Buckminsterfullerene," *Nature*, vol. 318, no. 6042, pp. 162-163, 1985.

[10] A. Mostofizadeh, Y. Li, B. Song, and Y. Huang, "Synthesis, properties, and applications of low-dimensional carbon-related nanomaterials," *Journal of Nanomaterials*, vol. 2011, 21 pages, 2011.

[11] N P I C, *The, "http://Nobelprize.org/,"*, 1996, 2022, http://nobelprize.org/nobel_prizes/chemistry/laureates/1996/.

[12] B. Kharisov and O. Kharissova, *Carbon Allotropes: Metal-Complex Chemistry, Properties and Applications*, Springer, 2019.

[13] S. Tiwari, V. Kumar, A. Huczko, R. Oraon, A. Adhikari, and G. Nayak, "Magical allotropes of carbon: prospects and applications," *Critical Reviews in Solid State and Materials Sciences*, vol. 41, no. 4, pp. 257–317, 2016.

[14] W. Krätschmer, L. Lamb, K. Fostiropoulos, and D. Huffman, "Solid C_{60}: a new form of carbon," *Nature*, vol. 347, no. 6291, pp. 354–358, 1990.

[15] S. Thakral and R. Mehta, "Fullerenes: an introduction and overview of their biological properties," *Indian Journal of Pharmaceutical Sciences*, vol. 68, no. 1, p. 13, 2006.

[16] P. Shanbogh and N. Sundaram, "Fullerenes revisited," *Resonance*, vol. 20, no. 2, pp. 123–135, 2015.

[17] A. Choudhary, "Fullerene chemistry an overview," *Ind. J. Res*, vol. 6, 2012.

[18] F. Sunqi, Z. Xing, W. En et al., "Superconductivity and structure of alkali-doped fullerenes: K_3C_{60} and Rb_3C_{60}," *Solid State Communications*, vol. 80, no. 8, pp. 639–642, 1991.

[19] M. Saunders, R. Cross, H. Jiménez-Vázquez, R. Shimshi, and A. Khong, "Noble gas atoms inside fullerenes," *Science*, vol. 271, no. 5256, pp. 1693–1697, 1996.

[20] G. Schick, A. Hirsch, H. Mauser, and T. Clark, "Opening and closure of the fullerene cage incis-bisimino adducts of C60: the influence of the addition pattern and the addend," *Chemistry–A European Journal*, vol. 2, no. 8, pp. 935–943, 1996.

[21] A. Hirsch and B. Nuber, "Nitrogen heterofullerenes," *Accounts of Chemical Research*, vol. 32, no. 9, pp. 795–804, 1999.

[22] L. Radushkevich and V. Lukyanovich, "About the structure of carbon formed by thermal decomposition of carbon monoxide on iron substrate," *J. Phys. Chem.(Moscow)*, vol. 26, pp. 88–95, 1952.

[23] A. Oberlin, M. Endo, and T. Koyama, "Filamentous growth of carbon through benzene decomposition," *Journal of Crystal Growth*, vol. 32, no. 3, pp. 335–349, 1976.

[24] S. Iijima, "Helical microtubules of graphitic carbon," *Nature*, vol. 354, no. 6348, pp. 56–58, 1991.

[25] J. Prasek, J. Drbohlavova, J. Chomoucka et al., "Methods for carbon nanotubes synthesis—review," *Journal of Materials Chemistry*, vol. 21, no. 40, pp. 15872–15884, 2011.

[26] R. Ding, G. Lu, Z. Yan, and M. Wilson, "Recent advances in the preparation and utilization of carbon nanotubes for hydrogen storage," *Journal of Nanoscience and Nanotechnology*, vol. 1, no. 1, pp. 7–29, 2001.

[27] Z. Tang, L. Zhang, N. Wang et al., "Superconductivity in 4 angstrom single-walled carbon nanotubes," *Science*, vol. 292, no. 5526, pp. 2462–2465, 2001.

[28] G. Rahman, Z. Najaf, A. Mehmood et al., "An overview of the recent progress in the synthesis and applications of carbon nanotubes," *Journal of Carbon Research*, vol. 5, no. 1, p. 3, 2019.

[29] F. Zhang, P. Hou, C. Liu, and H. Cheng, "Epitaxial growth of single-wall carbon nanotubes," *Carbon*, vol. 102, pp. 181–197, 2016.

[30] O. Zaytseva and G. Neumann, "Carbon nanomaterials: production, impact on plant development, agricultural and environmental applications," *Chemical and Biological Technologies in Agriculture*, vol. 3, no. 1, pp. 1–26, 2016.

[31] M. Lemme, *Current status of graphene transistors*, Trans Tech Publications Ltd, 2010.

[32] A. Adetayo and D. Runsewe, "Synthesis and fabrication of graphene and graphene oxide: a review," *Open Journal of Composite Materials*, vol. 9, no. 2, p. 207, 2019.

[33] A. Balandin, "Thermal properties of graphene and nanostructured carbon materials," *Nature Materials*, vol. 10, no. 8, pp. 569–581, 2011.

[34] K. Bolotin, K. Sikes, Z. Jiang et al., "Ultrahigh electron mobility in suspended graphene," *Solid State Communications*, vol. 146, no. 9-10, pp. 351–355, 2008.

[35] Z. Wu, W. Ren, L. Gao et al., "Synthesis of graphene sheets with high electrical conductivity and good thermal stability by hydrogen arc discharge exfoliation," *ACS Nano*, vol. 3, no. 2, pp. 411–417, 2009.

[36] R. Nair, P. Blake, A. Grigorenko et al., "Fine structure constant defines visual transparency of graphene," *Science*, vol. 320, no. 5881, pp. 1308–1308, 2008.

[37] C. Lee, X. Wei, J. Kysar, and J. Hone, "Measurement of the elastic properties and intrinsic strength of monolayer graphene," *Science*, vol. 321, no. 5887, pp. 385–388, 2008.

[38] K. Kim, Y. Zhao, H. Jang et al., "Large-scale pattern growth of graphene films for stretchable transparent electrodes," *Nature*, vol. 457, no. 7230, pp. 706–710, 2009.

[39] A. Smith, A. LaChance, S. Zeng, B. Liu, and L. Sun, "Synthesis, properties, and applications of graphene oxide/reduced graphene oxide and their nanocomposites," *Nano Materials Science*, vol. 1, no. 1, pp. 31–47, 2019.

[40] H. Schniepp, J. Li, M. McAllister et al., "Functionalized single graphene sheets derived from splitting graphite oxide," *The Journal of Physical Chemistry B*, vol. 110, no. 17, pp. 8535–8539, 2006.

[41] J. Paredes, S. Villar-Rodil, P. Solís-Fernández, A. Martínez-Alonso, and J. Tascon, "Atomic force and scanning tunneling microscopy imaging of graphene nanosheets derived from graphite oxide," *Langmuir*, vol. 25, no. 10, pp. 5957–5968, 2009.

[42] G. Eda and M. Chhowalla, "Chemically derived graphene oxide: towards large-area thin-film electronics and optoelectronics," *Advanced Materials*, vol. 22, no. 22, pp. 2392–2415, 2010.

[43] H. Sun, L. Wu, W. Wei, and X. Qu, "Recent advances in graphene quantum dots for sensing," *Materials Today*, vol. 16, no. 11, pp. 433–442, 2013.

[44] A. Stergiou, G. Pagona, and N. Tagmatarchis, "Donor–acceptor graphene-based hybrid materials facilitating photoinduced electron-transfer reactions," *Beilstein Journal of Nanotechnology*, vol. 5, no. 1, pp. 1580–1589, 2014.

[45] M. Mojica, J. Alonso, and F. Méndez, "Synthesis of fullerenes," *Journal of Physical Organic Chemistry*, vol. 26, no. 7, pp. 526–539, 2013.

[46] J. Guo, X. Wang, Y. Yao, X. Yang, X. Liu, and B. Xu, "Structure of nanocarbons prepared by arc discharge in water," *Materials Chemistry and Physics*, vol. 105, no. 2-3, pp. 175–178, 2007.

[47] T. Ikegami, F. Nakanishi, M. Uchiyama, and K. Ebihara, "Optical measurement in carbon nanotubes formation by pulsed laser ablation," *Thin Solid Films*, vol. 457, no. 1, pp. 7–11, 2004.

[48] Y. Zhu, T. Lin, Q. Liu et al., "The effect of nickel content of composite catalysts synthesized by hydrothermal method on the preparation of carbon nanotubes," *Materials Science and Engineering: B*, vol. 127, no. 2-3, pp. 198–202, 2006.

[49] G. Kucukayan, R. Ovali, S. Ilday et al., "An experimental and theoretical examination of the effect of sulfur on the pyrolytically grown carbon nanotubes from sucrose-based solid state precursors," *Carbon*, vol. 49, no. 2, pp. 508–517, 2011.

[50] S. Niyogi, E. Bekyarova, M. Itkis, J. McWilliams, M. Hamon, and R. Haddon, "Solution properties of graphite and graphene," *Journal of the American Chemical Society*, vol. 128, no. 24, pp. 7720-7721, 2006.

[51] S. Kataria, S. Wagner, J. Ruhkopf et al., "Chemical vapor deposited graphene: from synthesis to applications," *Physica Status Solidi A*, vol. 211, no. 11, pp. 2439–2449, 2014.

[52] M. Vittori Antisari, D. Gattia, L. Brandão, R. Marazzi, and A. Montone, *Carbon nanostructures produced by an AC arc discharge*, vol. 638-642, Trans Tech Publications Ltd, 2010.

[53] Z. Yang and J. Hao, "Progress in pulsed laser deposited two-dimensional layered materials for device applications," *Journal of Materials Chemistry C*, vol. 4, no. 38, pp. 8859–8878, 2016.

[54] A. Cano-Marquez, F. Rodriguez-Macias, J. Campos-Delgado et al., "Ex-MWNTs: graphene sheets and ribbons produced by lithium intercalation and exfoliation of carbon nanotubes," *Nano Letters*, vol. 9, no. 4, pp. 1527–1533, 2009.

[55] N. Zaaba, K. Foo, U. Hashim, S. Tan, W. Liu, and C. Voon, "Synthesis of graphene oxide using modified hummers method: solvent influence," *Procedia Engineering*, vol. 184, pp. 469–477, 2017.

[56] S. Horiuchi, T. Gotou, M. Fujiwara, T. Asaka, T. Yokosawa, and Y. Matsui, "Single graphene sheet detected in a carbon nanofilm," *Applied Physics Letters*, vol. 84, no. 13, pp. 2403–2405, 2004.

[57] P. Kyesmen, A. Onoja, and A. Amah, *Fullerenes synthesis by combined resistive heating and arc discharge techniques*, Springer Plus, 2016.

[58] A. Szabó, C. Perri, A. Csató, G. Giordano, D. Vuono, and J. Nagy, "Synthesis methods of carbon nanotubes and related materials," *Materials*, vol. 3, no. 5, pp. 3092–3140, 2010.

[59] A. Eatemadi, H. Daraee, H. Karimkhanloo et al., "Carbon nanotubes: properties, synthesis, purification, and medical applications," *Nanoscale Research Letters*, vol. 9, no. 1, pp. 1–13, 2014.

[60] M. Charlse and C. Chia-Chun, "Preparation of fullerenes and fullerene-based materials," *Solid State Phys.*, vol. 48, pp. 109–148, 1994.

[61] C. Rao, K. Subrahmanyam, H. Matte et al., "A study of the synthetic methods and properties of graphenes," *Science and Technology of Advanced Materials*, vol. 11, 2010.

[62] N. Li, Z. Wang, K. Zhao, Z. Shi, Z. Gu, and S. Xu, "Synthesis of single-wall carbon nanohorns by arc-discharge in air and their formation mechanism," *Carbon*, vol. 48, no. 5, pp. 1580–1585, 2010.

[63] T. Guo, P. Nikolaev, A. Rinzler, D. Tomanek, D. Colbert, and R. Smalley, "Self-assembly of tubular fullerenes," *The Journal of Physical Chemistry*, vol. 99, no. 27, pp. 10694–10697, 1995.

[64] A. Thess, R. Lee, P. Nikolaev et al., "Crystalline ropes of metallic carbon nanotubes," *Science*, vol. 273, no. 5274, pp. 483–487, 1996.

[65] A. Rao, E. Richter, S. Bandow et al., "Diameter-selective Raman scattering from vibrational modes in carbon nanotubes," *Science*, vol. 275, no. 5297, pp. 187–191, 1997.

[66] S. Mortazavi, P. Parvin, and A. Reyhani, "Fabrication of graphene based on Q-switched Nd:YAG laser ablation of graphite target in liquid nitrogen," *Laser Physics Letters*, vol. 9, no. 7, pp. 547–552, 2012.

[67] S. Pearce, S. Henley, F. Claeyssens et al., "Production of nanocrystalline diamond by laser ablation at the solid/liquid interface," *Diamond and Related Materials*, vol. 13, no. 4-8, pp. 661–665, 2004.

[68] Y. Sun, B. Zhou, Y. Lin et al., "Quantum-sized carbon dots for bright and colorful photoluminescence," *Journal of the American Chemical Society*, vol. 128, no. 24, pp. 7756-7757, 2006.

[69] H. Asano, S. Muraki, H. Endo, S. Bandow, and S. Iijima, "Strong magnetism observed in carbon nanoparticles produced by the laser vaporization of a carbon pellet in hydrogen-containing Ar balance gas," *Journal of Physics: Condensed Matter*, vol. 22, no. 33, p. 334209, 2010.

[70] J. Chrzanowska, J. Hoffman, A. Małolepszy et al., "Synthesis of carbon nanotubes by the laser ablation method: effect of laser wavelength," *Physica Status Solidi (B)*, vol. 252, no. 8, pp. 1860–1867, 2015.

[71] A. Stramel, M. Gupta, H. Lee, J. Yu, and W. Edwards, "Pulsed laser deposition of carbon nanotube and polystyrene-carbon nanotube composite thin films," *Optics and Lasers in Engineering*, vol. 48, no. 12, pp. 1291–1295, 2010.

[72] F. Bonaccorso, C. Bongiorno, B. Fazio et al., "Pulsed laser deposition of multiwalled carbon nanotubes thin films," *Applied Surface Science*, vol. 254, no. 4, pp. 1260–1263, 2007.

[73] P. Russo, A. Hu, G. Compagnini, W. Duley, and N. Zhou, "Femtosecond laser ablation of highly oriented pyrolytic graphite: a green route for large-scale production of porous graphene and graphene quantum dots," *Nanoscale*, vol. 6, no. 4, pp. 2381–2389, 2014.

[74] G. Kiran, B. Chandu, S. Acharyya, S. Rao, and V. Srikanth, "One-step synthesis of bulk quantities of graphene from graphite by femtosecond laser ablation under ambient conditions," *Philosophical Magazine Letters*, vol. 97, no. 6, pp. 229–234, 2017.

[75] J. Lehman, R. Deshpande, P. Rice, To B, and A. Dillon, "Carbon multi-walled nanotubes grown by HWCVD on a pyroelectric detector," *Infrared Physics & Technology*, vol. 47, no. 3, pp. 246–250, 2006.

[76] T. Makris, R. Giorgi, N. Lisi et al., "Carbon nanotubes growth by HFCVD: effect of the process parameters and catalyst preparation," *Diamond and Related Materials*, vol. 13, no. 2, pp. 305–310, 2004.

[77] Y. Choi, D. Bae, Y. Lee et al., "Growth of carbon nanotubes by microwave plasma-enhanced chemical vapor deposition at low temperature," *Journal of Vacuum Science & Technology A: Vacuum, Surfaces, and Films*, vol. 18, no. 4, pp. 1864–1868, 2000.

[78] H. Byon, H. Lim, H. Song, and H. Choi, "A synthesis of high purity single-walled carbon nanotubes from small diameters of cobalt nanoparticles by using oxygen-assisted chemical vapor deposition process," *Bulletin of the Korean Chemical Society*, vol. 28, no. 11, pp. 2056–2060, 2007.

[79] S. Kleckley, H. Wang, I. Oladeji et al., "Fullerenes and polymers produced by the chemical vapor deposition method," in *Synthesis and Characterization of Advanced Materials; ACS Symposium Series; American Chemical Society*, pp. 6–51, Washington, DC, USA, 1997.

[80] J. Kang, K. Qin, H. Zhang et al., "Direct synthesis of fullerene-intercalated porous carbon nanofibers by chemical vapor deposition," *Carbon*, vol. 50, no. 14, pp. 5162–5166, 2012.

[81] Y. Yang, X. Liu, X. Guo, H. Wen, and B. Xu, "Synthesis of nano onion-like fullerenes by chemical vapor deposition

using an iron catalyst supported on sodium chloride," *Journal of Nanoparticle Research*, vol. 13, no. 5, pp. 1979–1986, 2011.

[82] W. Choi, I. Lahiri, R. Seelaboyina, and Y. Kang, "Synthesis of graphene and its applications: a review," *Critical Reviews in Solid State and Materials Sciences*, vol. 35, no. 1, pp. 52–71, 2010.

[83] Y. Sun, Q. Wu, and G. Shi, "Graphene based new energy materials," *Energy & Environmental Science*, vol. 4, no. 4, pp. 1113–1132, 2011.

[84] J. Lee, H. Jeong, and W. Park, "Large-scale synthesis of graphene films by joule-heating-induced chemical vapor deposition," *Journal of Electronic Materials*, vol. 39, no. 10, pp. 2190–2195, 2010.

[85] J. Qi, W. Zheng, X. Zheng, X. Wang, and H. Tian, "Relatively low temperature synthesis of graphene by radio frequency plasma enhanced chemical vapor deposition," *Applied Surface Science*, vol. 257, no. 15, pp. 6531–6534, 2011.

[86] M. Yoon, S. Yang, E. Wang, and Z. Zhang, "Charged fullerenes as high-capacity hydrogen storage media," *Nano Letters*, vol. 9, no. 7, pp. 2578–2583, 2007.

[87] M. Yoon, S. Yang, C. Hicke, E. Wang, D. Geohegan, and Z. Zhang, "Calcium as the superior coating metal in functionalization of carbon fullerenes for high-capacity hydrogen storage," *Physical Review Letters*, vol. 100, no. 20, 2008.

[88] H. Dong, T. Hou, S. Lee, and Y. Li, "New Ti-decorated B_{40} fullerene as a promising hydrogen storage material," *Scientific Reports*, vol. 5, no. 1, pp. 1–8, 2015.

[89] X. Li and B. Wei, "Supercapacitors based on nanostructured carbon," *Nano Energy*, vol. 2, no. 2, pp. 159–173, 2013.

[90] Y. Shen, J. Reparaz, M. Wagner et al., "Assembly of carbon nanotubes and alkylated fullerenes: nanocarbon hybrid towards photovoltaic applications," *Chemical Science*, vol. 2, no. 11, pp. 2243–2250, 2011.

[91] J. Ma, Q. Guo, H. Gao, and X. Qin, "Synthesis of C60/graphene composite as electrode in supercapacitors," *Fullerenes, Nanotubes, and Carbon Nanostructures*, vol. 23, no. 6, pp. 477–482, 2015.

[92] H. Wang, X. Yan, and G. Piao, "A high-performance supercapacitor based on fullerene C_{60} whisker and polyaniline emeraldine base composite," *Electrochimica Acta*, vol. 231, pp. 264–271, 2017.

[93] R. Loutfy and S. Katagiri, "Fullerene materials for lithium-ion battery applications," in *In Perspectives of fullerene nanotechnology*, pp. 357–367, Dordrecht, Springer, 2002.

[94] J. Hosseini, A. Rastgou, and R. Moradi, "F-encapsulated $B_{12}N_{12}$ fullerene as an anode for Li-ion batteries: a theoretical study," *Journal of Molecular Liquids*, vol. 225, pp. 913–918, 2017.

[95] P. Sood, K. Kim, and S. Jang, "Electrochemical properties of boron-doped fullerene derivatives for lithium-ion battery applications," *ChemPhysChem*, vol. 19, no. 6, pp. 753–758, 2018.

[96] K. Tanigaki, T. Ebbesen, S. Saito et al., "Superconductivity at 33 K in $Cs_xRb_yC_{60}$," *Nature*, vol. 352, no. 6332, pp. 222-223, 1991.

[97] A. Kortan, "Superconductivity at 18 K in potassium-doped C60," *Nature*, vol. 350, 1991.

[98] A. Kumar, "Superconductivity of fullerenes: a review," *Research Journal Of Pharmaceutical Biological And Chemical Sciences*, vol. 8, no. 3, pp. 1045–1053, 2017.

[99] A. Mills and S. Le Hunte, "An overview of semiconductor photocatalysis," *Journal of Photochemistry and Photobiology A: Chemistry*, vol. 108, no. 1, pp. 1–35, 1997.

[100] Y. Yan, J. Miao, Z. Yang et al., "Carbon nanotube catalysts: recent advances in synthesis, characterization and applications," *Chemical Society Reviews*, vol. 44, no. 10, pp. 3295–3346, 2015.

[101] A. Kongkanand and P. Kamat, "Electron storage in single wall carbon nanotubes. Fermi level equilibration in semiconductor–SWCNT suspensions," *ACS Nano*, vol. 1, no. 1, pp. 13–21, 2007.

[102] M. Shaban, A. Ashraf, and M. Abukhadra, "TiO_2 nanoribbons/carbon nanotubes composite with enhanced photocatalytic activity; fabrication, characterization, and application," *Scientific Reports*, vol. 8, no. 1, pp. 1–17, 2018.

[103] A. Kamil, H. Mohammed, A. Balakit, F. Hussein, D. Bahnemann, and G. El-Hiti, "Synthesis, characterization and photocatalytic activity of carbon nanotube/titanium dioxide nanocomposites," *Arabian Journal for Science and Engineering*, vol. 43, no. 1, pp. 199–210, 2018.

[104] C. Kim, S. Hwang, J. Kim, and K. Yoo, "Photoelectrochemical cells using metal-decorated carbon nanotube electrodes," *Current Applied Physics*, vol. 10, no. 1, pp. 153–157, 2010.

[105] J. Kim, J. Jang, D. Youn, J. Kim, E. Kim, and J. Lee, "Graphene–carbon nanotube composite as an effective conducting scaffold to enhance the photoelectrochemical water oxidation activity of a hematite film," *RSC Advances*, vol. 2, no. 25, pp. 9415–9422, 2012.

[106] L. Wei, N. Tezuka, T. Umeyama, H. Imahori, and Y. Chen, "Formation of single-walled carbon nanotube thin films enriched with semiconducting nanotubes and their application in photoelectrochemical devices," *Nanoscale*, vol. 3, no. 4, pp. 1845–1849, 2011.

[107] W. Li, C. Liang, W. Zhou et al., "Preparation and characterization of multiwalled carbon nanotube-supported platinum for cathode catalysts of direct methanol fuel cells," *The Journal of Physical Chemistry B*, vol. 107, no. 26, pp. 6292–6299, 2003.

[108] L. Yang, S. Jiang, Y. Zhao et al., "Boron-doped carbon nanotubes as metal-free electrocatalysts for the oxygen reduction reaction," *Angewandte Chemie International Edition*, vol. 50, no. 31, pp. 7132–7135, 2011.

[109] K. Gong, F. Du, Z. Xia, M. Durstock, and L. Dai, "Nitrogen-doped carbon nanotube arrays with high electrocatalytic activity for oxygen reduction," *Science*, vol. 323, no. 5915, pp. 760–764, 2009.

[110] S. Paek, E. Yoo, and I. Honma, "Enhanced cyclic performance and lithium storage capacity of SnO_2/graphene nanoporous electrodes with three-dimensionally delaminated flexible structure," *Nano Letters*, vol. 9, no. 1, pp. 72–75, 2009.

[111] D. Wang, D. Choi, J. Li et al., "Self-assembled TiO_2–graphene hybrid nanostructures for enhanced Li-ion insertion," *ACS Nano*, vol. 3, no. 4, pp. 907–914, 2009.

[112] N. Li, Z. Chen, W. Ren, F. Li, and H. Cheng, "Flexible graphene-based lithium ion batteries with ultrafast charge and discharge rates," *Proceedings of the National Academy of Sciences*, vol. 109, no. 43, pp. 17360–17365, 2012.

[113] T. Mahmoudi, Y. Wang, and Y. Hahn, "Graphene and its derivatives for solar cells application," *Nano Energy*, vol. 47, pp. 51–65, 2018.

[114] B. Aissa, N. Memon, A. Ali, and M. Khraisheh, "Recent progress in the growth and applications of graphene as a smart material: a review," *Frontiers in Materials*, vol. 2, 2015.

[115] M. Choe, B. Lee, G. Jo et al., "Efficient bulk-heterojunction photovoltaic cells with transparent multi-layer graphene electrodes," *Organic Electronics*, vol. 11, no. 11, pp. 1864–1869, 2010.

[116] Q. Liu, Z. Liu, X. Zhang et al., "Organic photovoltaic cells based on an acceptor of soluble graphene," *Applied Physics Letters*, vol. 92, no. 22, 2008.

[117] Z. Liu, D. He, Y. Wang, H. Wu, and J. Wang, "Solution-processable functionalized graphene in donor/acceptor-type organic photovoltaic cells," *Solar Energy Materials and Solar Cells*, vol. 94, no. 7, pp. 1196–1200, 2010.

[118] K. Ukhurebor, R. Onyancha, U. Aigbe et al., "A methodical review on the applications and potentialities of using nano-biosensors for diseases diagnosis," *BioMed Reserach International*, vol. 2022, pp. 1–20, 2022.

[119] R. Kerry, K. Ukhurebor, S. Kumari et al., "A comprehensive review on the applications of nano-biosensor-based approaches for non-communicable and communicable disease detection," *Biomaterials Science*, vol. 9, no. 10, pp. 3576–3602, 2021.

[120] U. Aigbe, K. Ukhurebor, R. Onyancha et al., "A facile review on the sorption of heavy metals and dyes using bionanocomposites," *Adsorption Science & Technology*, vol. 2022, pp. 1–36, 2022.

[121] F. Perreault, A. De Faria, and M. Elimelech, "Environmental applications of graphene-based nanomaterials," *Chemical Society Reviews*, vol. 44, no. 16, pp. 5861–5896, 2015.

[122] F. Schedin, A. Geim, S. Morozov et al., "Detection of individual gas molecules adsorbed on graphene," *Nature Materials*, vol. 6, no. 9, pp. 652–655, 2007.

[123] J. Fowler, M. Allen, V. Tung, Y. Yang, R. Kaner, and B. Weiller, "Practical chemical sensors from chemically derived graphene," *ACS Nano*, vol. 3, no. 2, pp. 301–306, 2009.

[124] C. Shan, H. Yang, J. Song, D. Han, A. Ivaska, and L. Niu, "Direct electrochemistry of glucose oxidase and biosensing for glucose based on graphene," *Analytical Chemistry*, vol. 81, no. 6, pp. 2378–2382, 2009.

[125] S. Alwarappan, A. Erdem, C. Liu, and C. Li, "Probing the electrochemical properties of graphene nanosheets for biosensing applications," *The Journal of Physical Chemistry C*, vol. 113, no. 20, pp. 8853–8857, 2009.

[126] K. Ukhurebor, U. Aigbe, R. Onyancha et al., "Modified Nanomaterials for Environmenatal Applications-Electrochemical Synthesis, Characterization, and Properties," in *Biosensing Applications of Electrode Materials*, O. Ama, S. Ray, and P. Osifo, Eds., pp. 187–231, Springer Nature, 2022.